60 Watts Broadband Push Pull RF Power Amplifier Using LTCC Technology

by

Ayman Jundi

A thesis
presented to the University of Waterloo
in fulfillment of the
thesis requirement for the degree of
Master of Applied Science
in
Electrical and Computer Engineering

Waterloo, Ontario, Canada, 2013

AUTHOR'S DECLARATION

I hereby declare that I am the sole author of this thesis. This is a true copy of the thesis, including any required final revisions, as accepted by my examiners.

I understand that my thesis may be made electronically available to the public.

Ayman Jundi

Abstract

The continuous increase in wireless usage forces an immense pressure on wireless communication in terms of increased demand and spectrum scarcity. Service providers for communication services had no choice but to allocate new parts of the spectrum and present new communication standards that are more spectrally efficient. Communication is not only limited to mobile phones but recently attention has been given to intelligent transportation systems (ITS) where cars will be given a significant place in the communication network. Vehicular Ad-Hoc Network (VANET) is already assigned a slice of the spectrum at 5.9GHz using the IEEE802.11p standard also known as Dedicated Short-Range Communication (DSRC); however, this assignment will have limited range and functionality at first, and users are expected to depend on existing wireless mobile channels for some services such as video streaming and car entertainment. Therefore, it is essential to integrate existing wireless mobile communication standards into the skeleton of ITS at launch and most probably permanently.

An investigation was carried out regarding the existing communication standards including wireless local area networks (WLAN) and it was found that frequency bands from 400MHz up to 6GHz are being used in various regions around the world. It is also noted that current state of the art transceivers are composed of several transmitter front-ends targeting certain bands and standards. However, the more standards to be supported the more components to be added and the higher the cost not to mention the limited space in mobile devices. Multimode Multiband (MMMB) transmitters are therefore proposed as a potential solution to the existing redundancy in the number of front-end paths in modern transmitters. Broadband amplifiers are an essential part of any MMMB transmitter and they are also among the most challenging especially for high power requirements. This work explains why single ended topologies with efficiencies higher than 50% have a fundamental bandwidth limit such that the highest frequency of operation must be lower than twice the lowest frequency of operation. Hence, Push-Pull amplifier topology is being proposed as it was found that it has inherent broadband capabilities exceeding those of other topologies with comparable efficiency. The major advantage of Push-Pull power amplifiers is its capability of isolating the even harmonics present in the even mode operation of a Push-Pull amplifier from the less critical odd mode harmonics and the fundamental frequency. This separation between even and odd signals comes from the inclusion of a Balun at the output of push-pull amplifiers. Such separation makes it possible to operate amplifiers beyond the existing limit of single ended power amplifiers. To prove the concept, several Baluns were designed and tested and a comparison was made between different topologies in

terms of balance, bandwidth and odd and even mode performances; moreover, to illustrate the concept a Push-Pull power amplifier design was implemented using the multilayer Low Temperature Co-fired Ceramics (LTCC) technology with a bandwidth ratio of more than 100%.

Acknowledgements

The author acknowledges the contribution of the Diva NSERC group present in the University of Waterloo for their early involvement in the project in terms of academic and financial support. The author also acknowledges the valuable support and services provided by CMC Microsystems which helped in the fabrication and design process.

Dedication

This work is dedicated to

family & Friends

Table of Contents

List of Figures

List of Tables

Chapter 1
Introduction

1.1 Motivation

The enormous demand for wireless services forced an expansion on the wireless spectra allocated for mobile and wireless communication. Not only new frequency bands were allocated but also the new expansion came with communication standards that use broader channel bandwidths. Some standards, such as the IEEE802.11g (also known as WLAN or Wi-Fi) supports a band around 2.4GHz. Later on the Wi-Fi standard was upgraded to IEEE802.11n to support two frequency bands around 2.4GHz and 5GHz. This upgrade came at a cost of requiring power amplifiers that can operate efficiently at both bands. Dual-Band power amplifiers were proposed for such applications. However, when considering the case of mobile phones which needs to support a multitude of bands and standards, a dual band Power Amplifier (PA) is not sufficient. For the case of mobile communication under the Wide Area Network (WAN) classification, some researchers proposed using a reconfigurable radio which is capable of adjusting its band of operation when needed. Unfortunately, reconfigurable PAs are not designed for operating over multiple bands at the same time such that if the user is, for example, using Wi-Fi at 2.4GHz and had a voice call over 950MHz then the power amplifier will fail in establishing both connections at the same time unless it was designed for that scenario.

The motivation of this project started as a study of communication gateways of Intelligent Transportation Systems (ITS). The study led us to construct a diagram Figure 1.1 showing all the communication scenarios that are expected to be present in ITS services. These communication standards were collected and classified based on application type and standard as shown in Table 1.1. Based on the study, a sketch of the transceiver diagram was drawn as shown in Figure 1.2. It was concluded that for applications where multiple frequency bands are required at the same time, a Multimode Multiband (MMMB) PA capable of operating over a wide range of frequencies and able to amplify multiple signals at the same time is needed. This MMMB PA is best utilized for the use with mobile communication standards and Wi-Fi covering the bands between 0.7GHz and 3GHz.

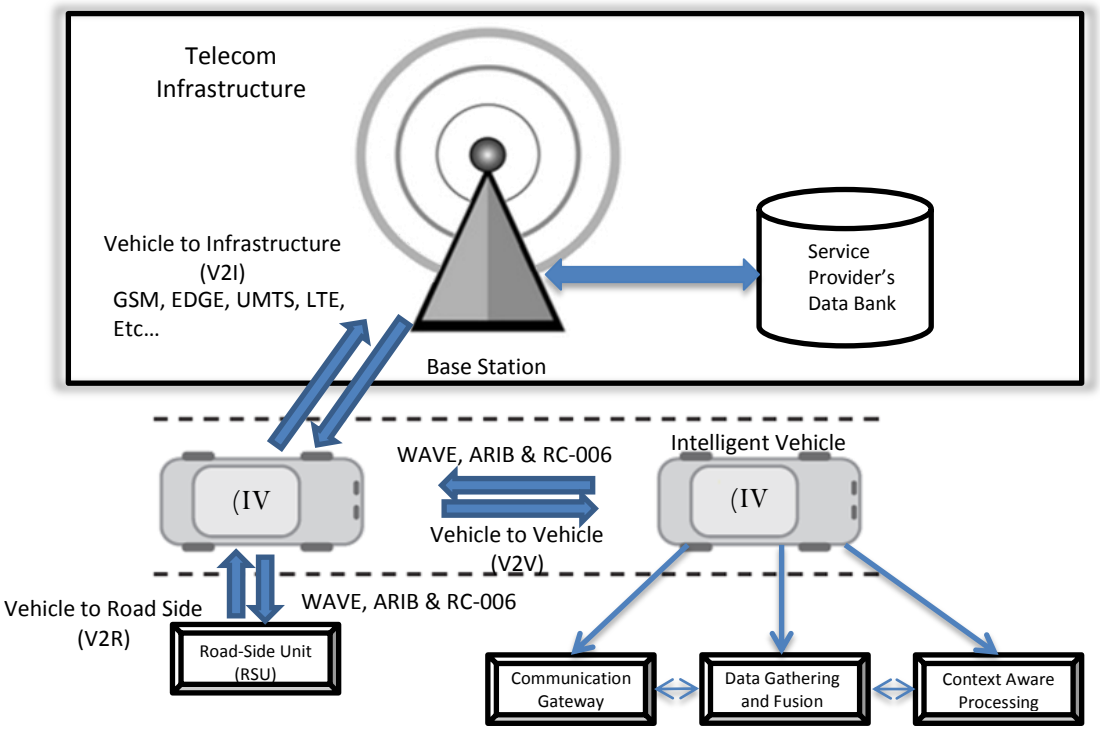

Figure 1.1: ITS communication standards diagram showing the various links an intelligent vehicle might establish with other nodes.

Table 1.1: Specifications of ITS communication Gateway classified per application and standard [1]

	DSRC			WAN			WLAN			
Standards	Wave	ARIB-T75	RC-006	GSM	UMTS	LTE	802.11 b	802.11 g	802.11 n	802.11 ac
Freq. Bands (MHz)	5850-5925	5770-5850	715-725	380-500 698-960, 1710-1991	410-500 716-960, 1710-2690	698- 960, 1427- 2200, 2500-2690	2400–2485	2400–2485	2400–2485, 4910-5835	5170-5835
Channel Bandwidth	10MHz, 20MHz	5MHz	10MHz	200KHz	5MHz-10MHz	5- 20MHz	22MHz	22MHz	20MHz, 40MHz	20MHz, 40MHz, 80MHz, 160MHz
Modulation	OFDM	ASK, QPSK	OFDM	GMSK	QPSK-64QAM	OFDM (DL), SC-FDMA(UL)	DSSS (DBSK, DQPSK)	OFDM	OFDM	OFDM
Multiple Access	CSMA	CSMA/ TS– CSMA	CSMA	TDMA	CDMA	SC- FDMA	CSMA	CSMA	CSMA	CSMA
Maximum Avg EIRP	33dBm	14.8dBm	20dBm	33dBm-39dBm	33dBm	23dBm	20dBm	17dBm	30dBm	30dBm
Max PAPR	~12dB	~6dB	~12dB	~0	~3.5dB	~8dB UL	~2.5dB	10dB<	10dB<	10dB<
EVM/ACPR	- 25dB/-	- /30dB @2.5MHz	- 25dB/-	-/- 60dB @400KHz	- /54dB @400KHz	- 22dB/-	-/- 30dB @20MHz	- 25dB/-	- 25dB/-	- 25dB/-

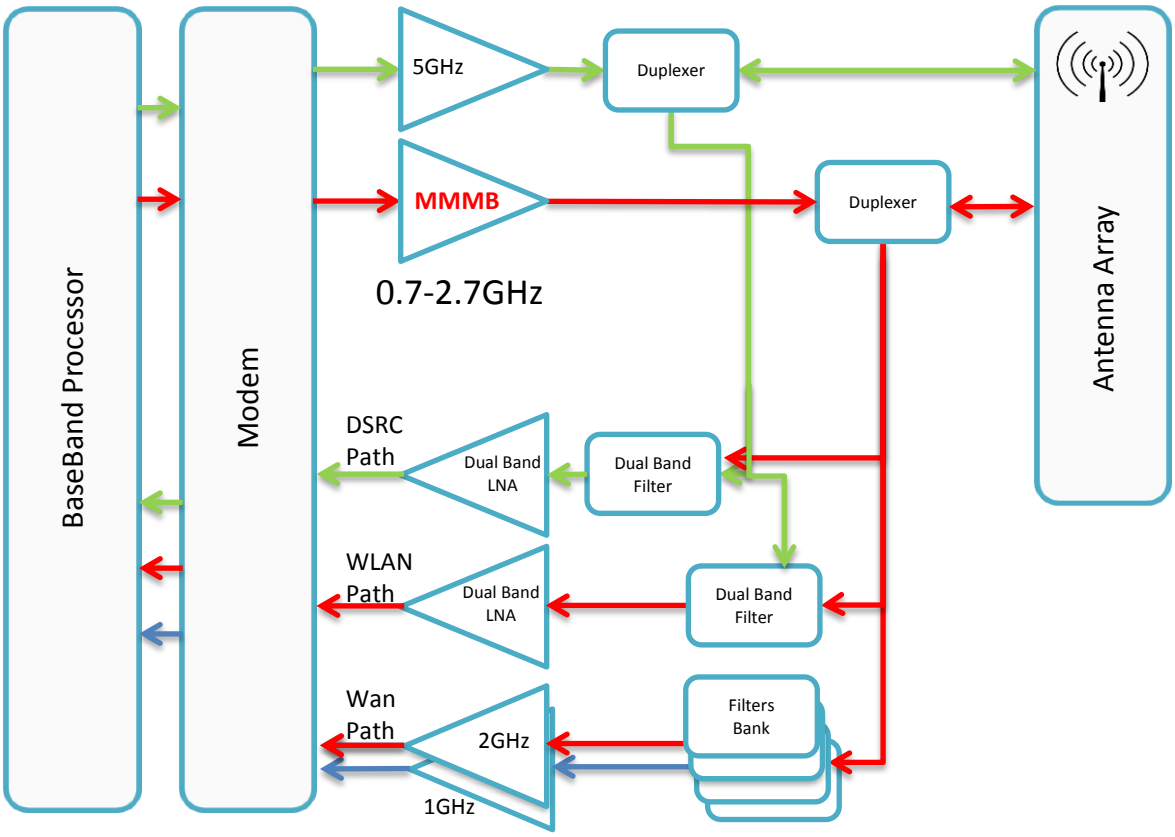

Figure 1.2: Proposed ITS communication Gateway transceiver topology employing an MMMB PA

The ITS communication gateway is expected to be able to handle a staggering number of frequency bands, communication standards, power levels and complex scenarios requiring two or even more concurrent wireless signal transmission. There are many challenges in designing a MMMB PA that can handle next generation requirements. These challenges include but are not limited to the following,

1. Achieving a satisfactory performance, such as high efficiency (at maximum power and back-off) and good gain, over a broad range of frequencies for instance from 700MHz to 2.7GHz.
2. Maintaining signal quality by providing linear operation and minimizing the interaction of multiple signals when transmitting them concurrently.
3. Being a compact and cost effective solution attractive to the industry.

The Push Pull topology is well established at low frequencies and it is the topology of choice when it comes to broadband and high efficiency applications. However, at Radio-Frequency (RF) operation the power splitting and combining mechanism are different than those at low frequency. This difference results in an unconventional behavior for the even mode waveforms which makes the design more difficult to maintain high efficiency and stable operation over broadband frequencies.

1.2 Thesis Organization

The thesis is organized as follows. Chapter 2 will outline the theory behind conventional power amplifier design illustrating the differences between different classes of operation. An ideal transistor model will be used to explain a simplified design methodology showing how the bias voltage and load termination affects the amplifier performance. Broadband operation will be explained through the introduction of the design space concept. Class B/J and the recently introduced continuous class F use the power amplifier design space concept to extend the possible range of impedances that provide theoretically identical performance to the conventional class B and Class F respectively. Finally, the Push-Pull topology will be presented as the topology best suited to design broadband and high efficiency amplifiers.

Chapter 3 will expand on the role of Baluns in Push-Pull amplifiers and how different topologies could affect the performance of the push-pull power amplifier. Firstly, a detailed Balun background will be presented introducing the ideal Balun and the three major Balun categories and elaborating on the difference between low frequency and high frequency Baluns. Then the most relevant Balun topologies in literature will be introduced and critically analyzed in the context of balance, bandwidth and practicality. Finally, measurement results will be shown for several fabricated Balun prototypes.

Chapter 4 will present the broadband push-pull power amplifier design procedure and simulation results. Firstly, the push-pull power amplifier design steps will be presented and the design choices will be explained and justified. Then the LTCC technology will be introduced and its advantages for our application will be highlighted. The design abstracted layouts and procedure will be illustrated and finally the simulation results of the whole design will be shown and criticized.

Finally, chapter 5 will conclude this work and present further possibilities to investigate in future works.

Chapter 2
Broadband Power Amplifiers

2.1 Introduction

This chapter will outline the theory behind conventional power amplifier design illustrating the differences between different classes of operation. An ideal transistor model will be used to explain a simplified design methodology showing how the bias voltage and load termination affects the amplifier performance. Broadband operation will be explained through the introduction of the design space concept. Class B/J and the recently introduced continuous class F use the design space concept to extend the possible range of impedances that provide theoretically identical performance to the conventional class B and Class F respectively. Finally, the Push-Pull topology will be presented as the topology best suited to design broadband and high efficiency amplifiers.

2.2 Ideal Transistor Model

In this chapter we will use an ideal transistor model to illustrate the various power amplifier classes and topologies mentioned in the previous section. The ideal transistor shown in Figure 2.1 consists of a voltage control current source with V_{gs} as the input voltage and I_{ds} as the output current. The current source operates linearly with input voltage levels above the pinch-off voltage V_p and below the saturation voltage as shown in Figure 2.2A. Moreover, the current source requires a positive voltage higher than the knee voltage V_k and lower than the breakdown voltage applied to its drain terminal. The DC-IV characteristics is shown in Figure 2.2B. The following simplified analysis assumes no parasitic elements associated with the transistor. This assumption is valid in the context of illustrating basic operation of various classes. The DC component of voltages and currents will be distinguished by capital letter subscripts and an average bar over the term while the AC or RF terms will have small letter subscripts. The terms with capital letter subscripts and no average bar denote the total signal.

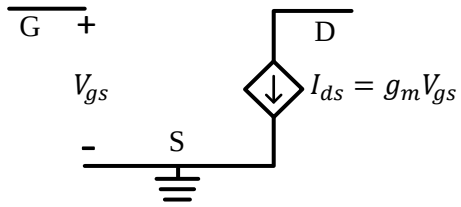

Figure 2.1: The ideal FET model

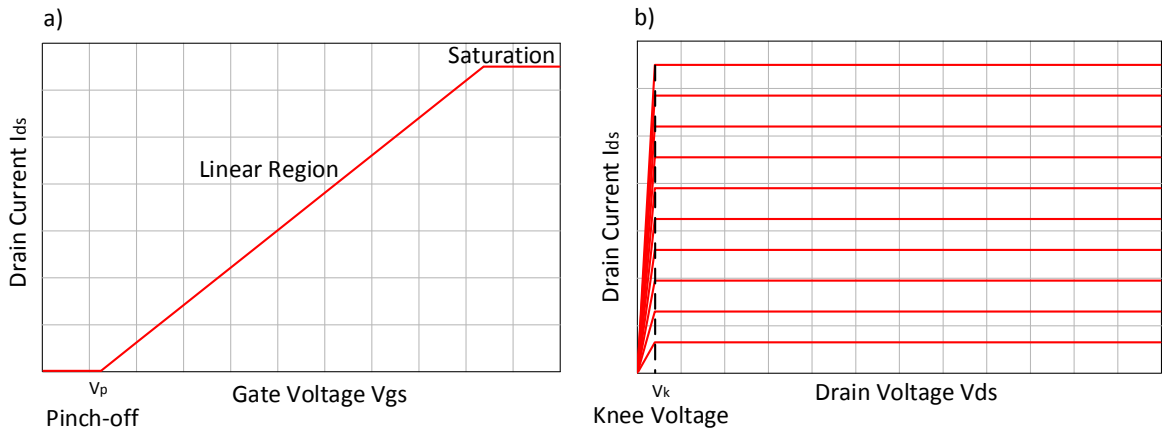

Figure 2.2: The characteristics of the ideal model a) V_{gs} to I_{ds} transfer characteristic b) I_{ds} vs. V_{ds} for varying V_{gs}

2.3 Conventional Power Amplifier Classes

2.3.1 Class A

Class A is the simplest class of operation of power amplifiers and is usually used as a benchmark for other classes. Class A is biased with a gate voltage in the middle of the region between the pinch-off and saturation such that the DC component of I_{DS} denoted by $\overline{I_{DS}}$ is half the maximum current provided by the transistor. On the other hand, the drain dc voltage is set as the average of the knee voltage and break down voltage. The input voltage is allowed to swing strictly between the pinch-off voltage and the saturation voltage while the output voltage is allowed to swing between the knee voltage and the breakdown voltage. The maximum power is achieved by aligning the maximum swing at the input with the maximum swing at the output using the proper output resistance denoted as R_{opt} [2]. Figure 2.3 shows the relation between input and output voltages.

The slope of the AC load line is set by the value of the load impedance and for maximum output power the value of the load impedance R_{opt} is given by,

$$R_{opt} = \frac{V_{max}}{I_{max}} = \frac{2\overline{V_{DS}}}{2\overline{I_{DS}}} = \frac{\overline{V_{DS}}}{\overline{I_{DS}}} \tag{2.1}$$

For this case the output power will be,

$$P_{out_{max}} = \frac{1}{2}\overline{V_{DS}} \times \overline{I_{DS}} = \frac{1}{8}V_{max} \times I_{max} \tag{2.2}$$

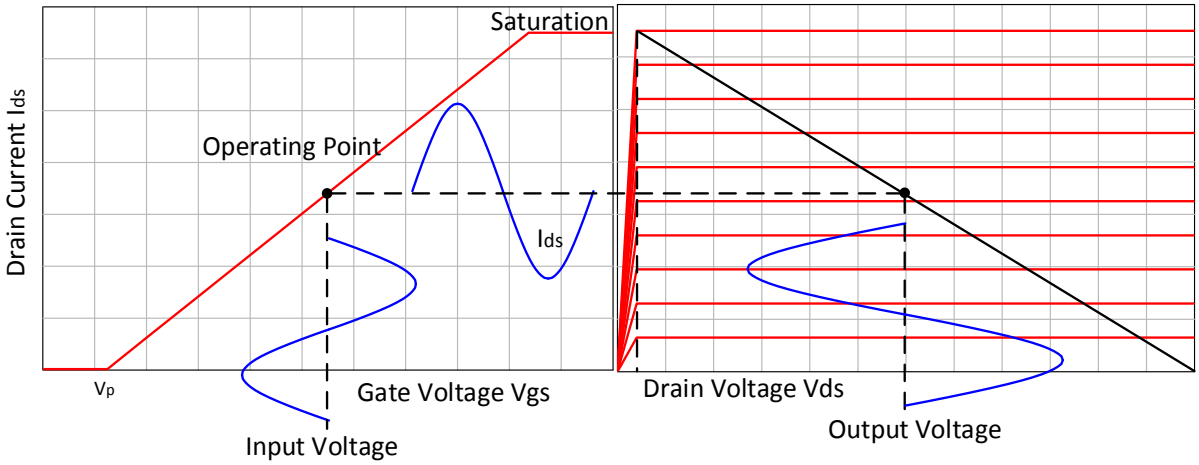

Figure 2.3: The relation between input and output waveforms of class A power amplifiers

One of the important metrics in power amplifier design is the efficiency. The efficiency of a power amplifier is the measure of how good it is in converting DC power into AC power and is measured as the ratio between output RF power and input DC power. There are two major ways to define an amplifier's efficiency and they are namely the Drain Efficiency (η) and the Power Added Efficiency (PAE). The two terms are related to each other such that the PAE is always less than the DE because it subtracts the input RF power from the output RF power. The two measures are illustrated in equations (2.3) and (2.4),

$$\eta = \frac{[P_{Out}]_{RF}}{[P_{in}]_{DC}} \times 100\% \tag{2.3}$$

$$PAE = \frac{[P_{Out}]_{RF} - [P_{in}]_{RF}}{[P_{in}]_{DC}} \times 100\% \tag{2.4}$$

In the case of class A operation the maximum efficiency happens at maximum output power and is computed as follows,

$$\eta = \frac{[P_{Out}]_{RF}}{[P_{in}]_{DC}} \times 100\% = \frac{\frac{1}{2}\overline{V_{DS}} \times \overline{I_{DS}}}{\overline{V_{DS}} \times \overline{I_{DS}}} \times 100\% = 50\% \tag{2.5}$$

Since the maximum theoretical efficiency for class A does not exceed 50% it not used for high efficiency application; however, class A provides the best linearity. The definition of linearity varies based on context and in the case of power amplifiers it is defined by the relation between input fundamental power and output fundamental real power. Linear power amplifiers do not produce any intermodulation products in theory; however, in practice there is always nonlinearity present. Therefore, the term "linear" is defined relative to the application requirements which is usually defined by certain standards. Due to the linearity of class A, it is still used in some applications where the signal quality is critical such as in preamplifiers and some military applications [2].

2.3.2 Class B

As mentioned previously class A amplifiers are biased such that DC power is dissipated even if there is no input. Class B amplifiers are biased with a gate voltage at pinch-off such that the transistor is not dissipating any current in the absence of an input signal i.e. $\overline{I_{DS}}$ is zero. The drain voltage $\overline{V_{DS}}$, however, is biased midway between the maximum voltage and the knee voltage just as in class A. The AC load-line is different than that of class A but it leads to the same maximum output power. The relation between input and output signals is shown in Figure 2.4 [2].

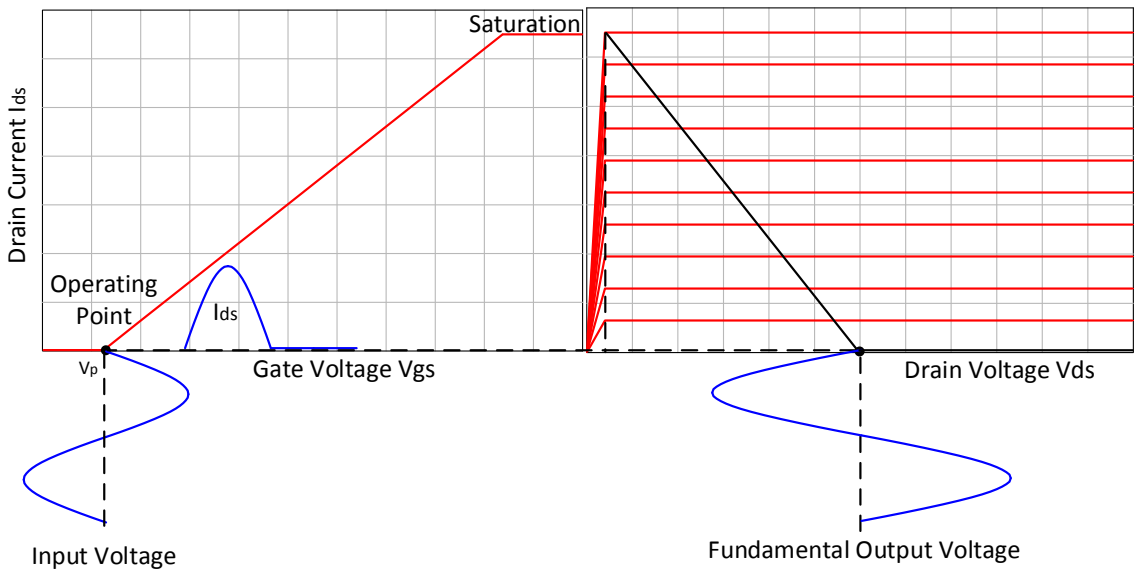

Figure 2.4: The relation between input and output waveforms of class B power amplifiers

Even though the maximum output power is the same as that of class A, class B power amplifiers need to be driven with four times as much input power to produce the same output power compared

to class A. Based on that, the power gain of class B power amplifiers is one quarter that of class A power amplifiers. Note that power gain (G) of a power amplifier is defined as follows,

$$G = \frac{[P_{Out}]_{RF}}{[P_{in}]_{RF}} \tag{2.6}$$

For a proper class B operation, higher order harmonics has to be shorted out in order to get maximum voltage swing over the fundamental frequency to produce the maximum output power at the fundamental frequency. This shorting of harmonics will lead to bandwidth limitations as will be discussed in later sections.

From the waveform of the current I_{DS} we can deduce the DC, fundamental and harmonic content using Fourier series expansion. By taking Fourier transform of the half sinusoid we get the following,

$$\overline{I_{DS}} = \frac{1}{2\pi}\int_{-\frac{\pi}{2}}^{\frac{\pi}{2}} \frac{I_{max}}{1-\cos\left(\frac{\pi}{2}\right)}\left[\cos(\theta) - \cos\left(\frac{\pi}{2}\right)\right] d\theta \tag{2.7}$$

$$I_{ds_n} = \frac{1}{\pi}\int_{-\frac{\pi}{2}}^{\frac{\pi}{2}} \frac{I_{max}}{1-\cos\left(\frac{\pi}{2}\right)}\left[\cos(\theta) - \cos\left(\frac{\pi}{2}\right)\right] \cos(n\theta)\, d\theta \tag{2.8}$$

Where, I_{ds_n} denotes the current amplitude of the nth harmonic. Note that the signal is assumed to be symmetric around the y-axis hence it does not contain any sine terms and it purely consist of cosine terms given that the function is even. If the function was not even then we would require an additional term to describe the signal fully. The DC component can be written in terms of I_{max} as,

$$\overline{I_{DS}} = \frac{1}{2\pi}\int_{-\frac{\pi}{2}}^{\frac{\pi}{2}} \frac{I_{max}}{1-\cos\left(\frac{\pi}{2}\right)}\left[\cos(\theta) - \cos\left(\frac{\pi}{2}\right)\right] d\theta \ = \frac{I_{max}}{\pi}\ A \tag{2.9}$$

While the amplitude of the fundamental can be written as,

$$I_{ds_1} = \frac{1}{\pi}\int_{-\frac{\pi}{2}}^{\frac{\pi}{2}} \frac{I_{max}}{1-\cos\left(\frac{\pi}{2}\right)}\left[\cos(\theta) - \cos\left(\frac{\pi}{2}\right)\right] \cos(\theta)\, d\theta \ = \frac{I_{max}}{2} \tag{2.10}$$

The efficiency of class B is computed by writing everything in terms of I_{max} and V_{max} as follows,

$$\eta = \frac{[P_{out}]_{RF}}{[P_{in}]_{DC}} \times 100\% = \frac{\frac{1}{2}\frac{V_{max}}{2} \times \frac{I_{max}}{2}}{\frac{V_{max}}{2} \times \frac{I_{max}}{\pi}} \times 100\% = \frac{\pi}{4} \times 100\% \cong 78.5\% \quad (2.11)$$

Class B power amplifiers are considered linear in terms of input and output power levels. This is in contradiction to other claims that can be found in literature. As mentioned in the previous section linearity in power amplifiers is not based on voltage and current waveforms but is based on the relation between input and output real power levels at the fundamental frequency. Even though class B operation produces harmonic content due to the fact that the current is half a sinusoid, it does not produce any intermodulation products unless the amplifier saturates and enters the knee region. However, in practice there are other non-idealities in the transistor, such as soft turn-on voltage and nonlinear g_m, which forces class B to behave nonlinearly [2].

2.3.3 Class AB

It was shown in the earlier section that by biasing the gate of the transistor exactly at pinch-off the maximum efficiency was enhanced beyond the 50% limit of class A. One might conclude that there should be a class of operation between class A and Class B where the gate is biased between those classes. Such a class is referred to as class AB.

Class AB power amplifiers is a way to compromise between the efficiency of class B and the linearity and gain of class A. As explained earlier, class B is nonlinear due to non-idealities of the transistor including the soft turn-on voltage; in class AB the nonlinearity is reduced by biasing the gate away from the pinch-off voltage, thus avoiding the nonlinearity due to the soft turn-on of the transistor. In order to explain the operation of class AB we need to explain the concept of conduction angle. The conduction angle (α) refers to the portion of the signal where the amplifier is turned on and conducting power. For instance, in class A the conduction angle is 2π since the amplifier is ON during the complete cycle of the input signal. In class B, however, the conduction angle is π since the transistor is ON only for the positive half of the sinusoidal signal. The current waveform can be written in terms of the conduction angle as follows [2],

$$I_{DS} = \begin{cases} \frac{I_{max}}{1 - \cos\left(\frac{\alpha}{2}\right)}\left[\cos(\theta) - \cos\left(\frac{\pi}{2}\right)\right] & -\frac{\alpha}{2} \leq \theta \leq \frac{\alpha}{2} \\ 0 & Otherwise \end{cases} \quad (2.12)$$

The comparison between the current waveforms for Classes A, B and AB is shown in Figure 2.5.

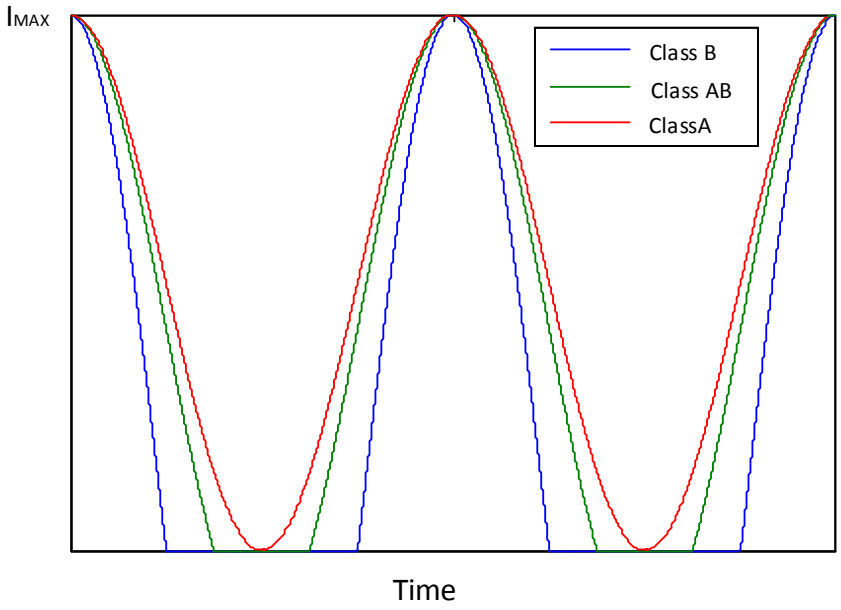

Figure 2.5: The comparison between the current waveforms for Classes A, B and AB

Based on the general term of the drain current we can deduce the DC and AC content using Fourier series expansion as given by,

$$\overline{I_{DS}} = \frac{1}{2\pi}\int_{-\frac{\alpha}{2}}^{\frac{\alpha}{2}} \frac{I_{max}}{1-\cos\left(\frac{\alpha}{2}\right)}\left[\cos(\theta)-\cos\left(\frac{\alpha}{2}\right)\right]d\theta \tag{2.13}$$

$$I_{ds_n} = \frac{1}{\pi}\int_{-\frac{\alpha}{2}}^{\frac{\alpha}{2}} \frac{I_{max}}{1-\cos\left(\frac{\alpha}{2}\right)}\left[\cos(\theta)-\cos\left(\frac{\alpha}{2}\right)\right]\cos(n\theta)\,d\theta \tag{2.14}$$

From Equations (2.13) and (2.14) we can deduce the maximum output power, gain and efficiency. The maximum power of class AB is higher than that of class A. This can be explained by looking at the magnitude of the fundamental component of I_{DS} normalized to that of class A. Note that the voltage does not have any harmonics aside from the fundamental since the load is forced to be a short-circuit starting from the second harmonic onwards. The relation between the fundamental current component and conduction angle is shown in Figure 2.6.

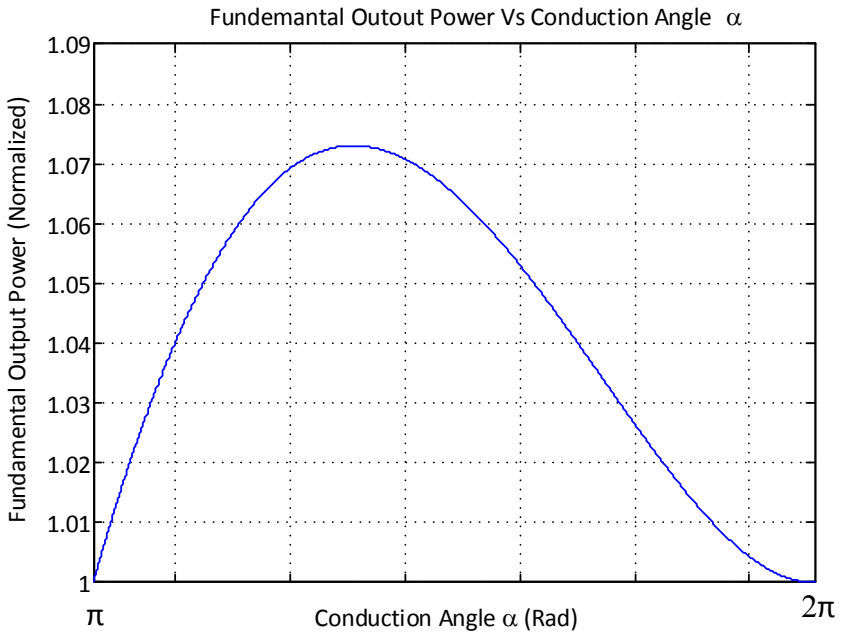

Figure 2.6: The normalized fundamental component of the output power given as a function of the conduction angle α in radians

Since the voltage swing is designed to be identical to that of class A then the increase in fundamental current will reflect to an increase in output power. The maximum output power happens at a conduction angle of $\alpha = 4.28\, rad$.

The normalized linear power Gain (G) is also a function of the conduction angle and is given by,

$$G = \frac{[P_{Out}]_{RF}}{[P_{in}]_{RF}} = \frac{[P_{Out}]_{RF\,ClassA} \times \frac{2}{\pi}\int_{-\frac{\alpha}{2}}^{\frac{\alpha}{2}} \frac{1}{1-\cos\left(\frac{\alpha}{2}\right)}\left[\cos(\theta) - \cos\left(\frac{\alpha}{2}\right)\right]\cos(\theta)\, d\theta}{[P_{in}]_{RF\,ClassA}\left(\frac{2}{1-cos\left(\frac{\alpha}{2}\right)}\right)^2} \qquad (2.15)$$

The efficiency is then computed based on the conduction angle at maximum power assuming all higher order harmonics are short circuited and V_{DS} is at full swing,

$$\eta = \frac{[P_{out}]_{RF}}{[P_{in}]_{DC}} \times 100\% = \frac{\frac{1}{2}\frac{V_{max}}{2} \times \frac{1}{\pi}\int_{-\frac{\alpha}{2}}^{\frac{\alpha}{2}} \frac{I_{max}}{1-\cos\left(\frac{\alpha}{2}\right)}\left[\cos(\theta) - \cos\left(\frac{\alpha}{2}\right)\right]\cos(\theta)\, d\theta}{\frac{V_{max}}{2} \times \frac{1}{2\pi}\int_{-\frac{\alpha}{2}}^{\frac{\alpha}{2}} \frac{I_{max}}{1-\cos\left(\frac{\alpha}{2}\right)}\left[\cos(\theta) - \cos\left(\frac{\alpha}{2}\right)\right] d\theta} \times 100\% \qquad (2.16)$$

$$\eta = \frac{\int_{-\frac{\alpha}{2}}^{\frac{\alpha}{2}}\left[\cos(\theta) - \cos\left(\frac{\alpha}{2}\right)\right]\cos(\theta)\, d\theta}{\int_{-\frac{\alpha}{2}}^{\frac{\alpha}{2}}\left[\cos(\theta) - \cos\left(\frac{\alpha}{2}\right)\right] d\theta} \times 100\% \qquad (2.17)$$

Figure 2.7 shows the efficiency and gain of class AB vs. the conduction angle. Note that the gain is normalized relative to class A.

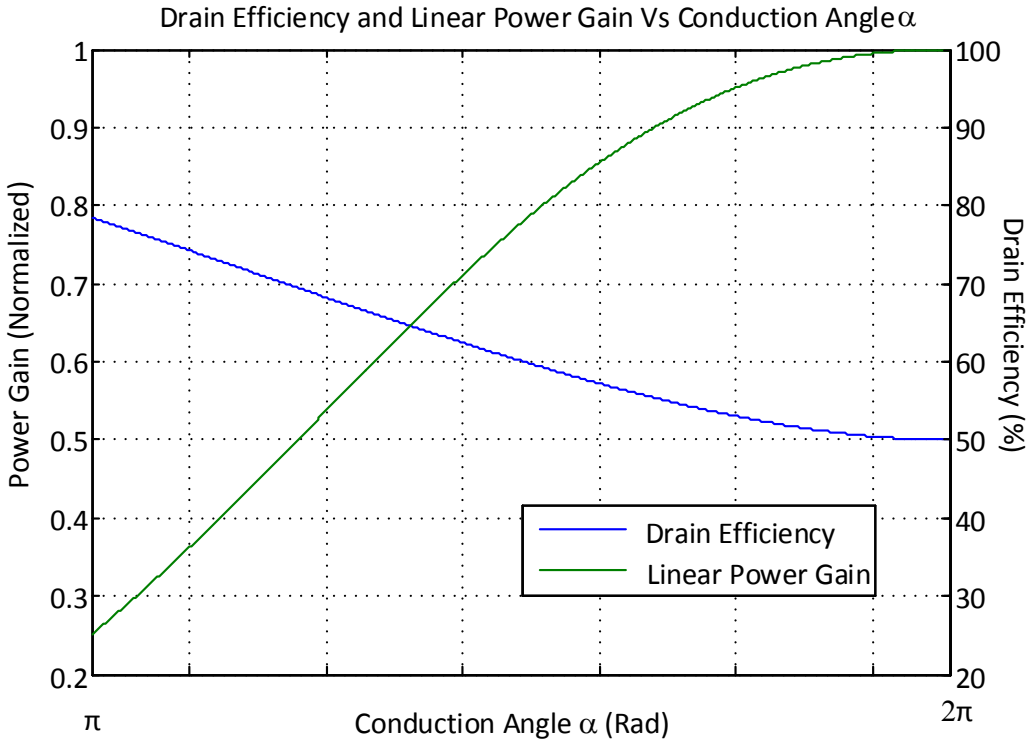

Figure 2.7: The Drain Efficiency and normalized power gain of class AB vs. the conduction angle

As mentioned before class B is considered theoretically linear when assuming and ideal transistor model. Under the same assumption, Class AB is not linear for all power levels. The reason being that for every input power the conduction angle is prone to change depending on the bias voltages and currents; from Figure 2.7 we can see that if the conduction angle changes the gain also changes leading to a nonlinear relation between the input and output fundamental powers. Yet in practice,

class AB is more linear than class B power amplifiers and there is no proper way to illustrate this using an ideal transistor model since the major contributor is the nonlinear device characteristics that are technology dependent [2].

2.3.4 Class C

Amplifiers biased in class B or class AB operate in a mode known as reduced conduction angle mode. Another variation on reduced conduction angle mode is class C power amplifiers. Class C has a gate bias voltage below the pinch-off voltage to further increase the ratio of the fundamental component to the DC component of I_{DS} hence increasing the efficiency of the power amplifier. The conduction angle of class C is below π which means that the transistor does not conduct energy for more than half the time. Equations (2.13) and (2.14) introduced in the previous section apply for all values of α and can be used to plot the output power, gain and efficiency equations for Class C as shown in Figure 2.8.

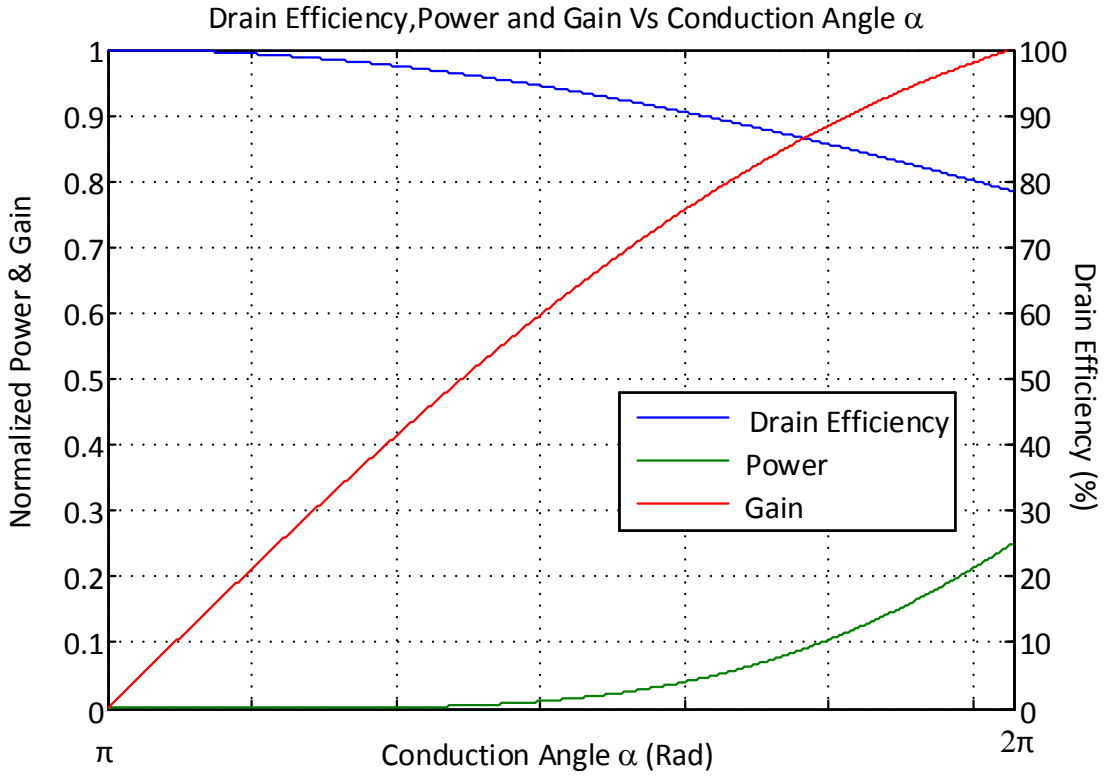

Figure 2.8: The drain efficiency, normalized output power and normalized Gain as a function of the conduction angle α

Regardless of the potential high efficiency of class C, it suffers from major drawbacks. This class of operation is highly nonlinear and it does not amplify any signal below a certain threshold usually decided by the gate's bias voltage. The maximum output power is lower than that of class A and the gain declines rapidly rendering the amplifier unusable at very low conduction angles. Other classes of operation such as class F/F^{-1} were later introduced to overcome these limitations [2].

2.4 High efficiency Harmonically Tuned Amplifiers

2.4.1 Class *F/F* $^{-1}$

Class F is a reduced conduction angle class of operation with harmonic tuning added to minimize the power dissipated by the transistor; hence, reducing wasted power and increasing efficiency. The ideal waveforms of class F power amplifiers are shown in Figure 2.9 illustrating the main concept. It can be noticed that the voltage and current waveforms do not overlap at any point in time; hence, the power dissipation through the transistor is theoretically zero.

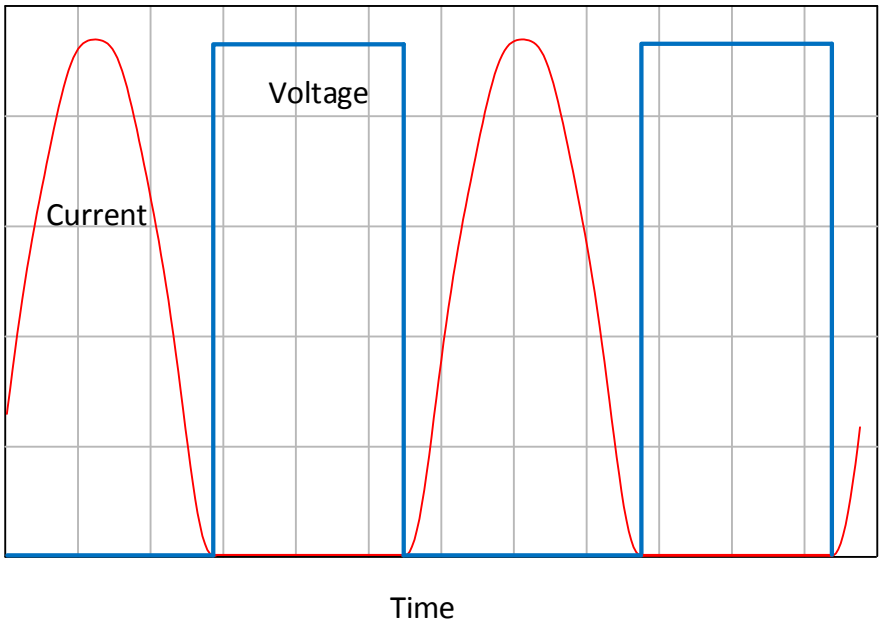

Figure 2.9: The theoretical current and voltage waveforms for class F power amplifier operating at 100% Drain efficiency

The Fourier series expansion can be written for both the voltage and current waveforms as follows,

$$I_{DS} = I_{max}\left[\frac{1}{\pi} + \frac{1}{2}\sin(\omega t) - \frac{1}{\pi}\sum_{\substack{n=2 \\ Even}}^{\infty}\left(\frac{\cos(n\omega t)}{n^2-1}\right)\right] \tag{2.18}$$

$$V_{DS} = V_{max}\left[\frac{1}{2} - \frac{2}{\pi}\sum_{\substack{n=1 \\ Odd}}^{\infty}\left(\frac{\sin(n\omega t)}{n}\right)\right] \tag{2.19}$$

From the waveforms, it can be deduced that the load terminations needed to synthesize them. The absence of odd current harmonics in the current waveform points to the presence of open circuit termination for odd harmonics other than the fundamental. Similarly the absence of even harmonics in the voltage waveform points to a short circuit termination for all even harmonics. From (2.20) and (2.21), it is possible to compute the efficiency and output power of Class F power amplifiers and they are as follows,

$$\eta = \frac{[P_{out}]_{RF}}{[P_{in}]_{DC}} \times 100\% = \frac{0.5 \times 2V_{max}/\pi \times I_{max}/2}{V_{max}/2 \times I_{max}/\pi} \times 100\% = 100\% \tag{2.20}$$

$$[P_{out}]_{RF} = \frac{1}{2}\frac{2V_{max}}{\pi}\frac{I_{max}}{2} = \frac{4}{\pi}\left(\frac{1}{2}\frac{V_{max}}{2} \times \frac{I_{max}}{2}\right) = \frac{4}{\pi}[P_{out}]_{RF\,ClassA} \tag{2.21}$$

In practice, an infinite number of terminations for all the harmonics is not possible to achieve; therefore, most designs only include terminations up to the third harmonic. The theoretical maximum efficiency achievable depends on the number of harmonics that are terminated properly. Table 2.1 lists the efficiency and output power achievable with the number of harmonic terminations introduced to the voltage waveform when the current waveform is assumed to be half a sinusoid and the voltages are normalized to V_{MAX} [2].

Table 2.1: The optimal voltage components maximizing V1 for (m) odd order terminations [2]

m	V_1	V_3	V_5	V_7	**Normalized** P_{out} (dB)	μ (%)
1	1	-	-	-	0	78.5
2	1.155	0.1925	-	-	0.625	90.7
3	1.207	0.2807	0.073	-	0.82	94.8
4	1.231	0.3265	0.123	0.0359	0.90	96.7
∞	1.273	0.4244	0.2546	0.1819…	1.05	100

Class F^{-1}, also known as inverse class F, operates in a very similar fashion except that the waveforms are interchanged leading to inverted harmonic terminations Figure 2.10.

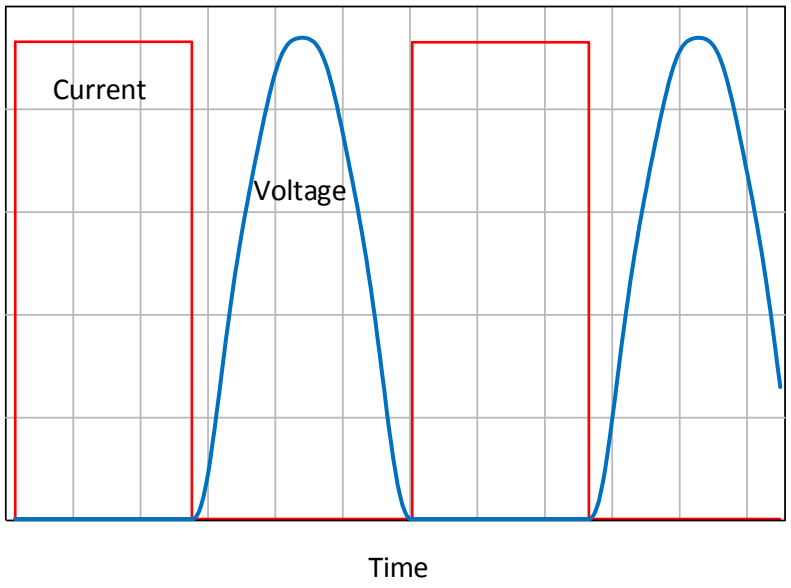

Figure 2.10: The theoretical current and voltage waveforms for class F^{-1} power amplifier operating at 100% Drain efficiency

One of the main differences between class F and inverse class F is that practical implementation of Class F^{-1} has higher output power with limited number of harmonic terminations. This is due to the fact that it is operates in an overdriven mode to produce the square shape of the current waveform. Table 2.2 shows the efficiency and output power achievable by class F^{-1} given the number of harmonic terminations of the voltage waveform where the voltages are normalized to V_{MAX} .

Table 2.2: The optimal voltage components minimizing the DC component for (n) even order terminations [2]

n	V_0	V_1	V_2	V_4	Normalized P_{out} (dB)	μ (%)
1	0.5	0.5	-	-	1.05	63.6
2	0.375	0.5	0.125	-	1.05	84.8
3	0.334	0.5	0.193	0.026	1.05	95.4
∞	0.318	0.5	0.2122	0.0424 …	1.05	100

2.5 Broadband Power amplifiers

2.5.1 Class B/J

2.5.1.1 Sensitivity of Class B

Conventional class B power amplifier requires a short circuit termination for all the higher order harmonics. However, most practical class B amplifiers focus only on terminating the second harmonic with a short circuit ignoring the higher order harmonics. In broadband power amplifiers a broadband short circuit for the second harmonic limits the bandwidth of operation since providing a broadband short circuit is very challenging for frequencies higher than 1GHz. In order to study the sensitivity of class B to the short circuit termination the following experiment was performed. The fundamental impedance was kept constant at R_{opt} while the phase of the second harmonic termination was varied**Error! Reference source not found.**. It was evident that the efficiency will egrade for the same input power as the second harmonic termination shifts into other loads Figure 2.12. The reason was attributed to the fact that the voltage is then forced beyond the knee region and the current is chocked as a result of the low voltage Figure 2.13.

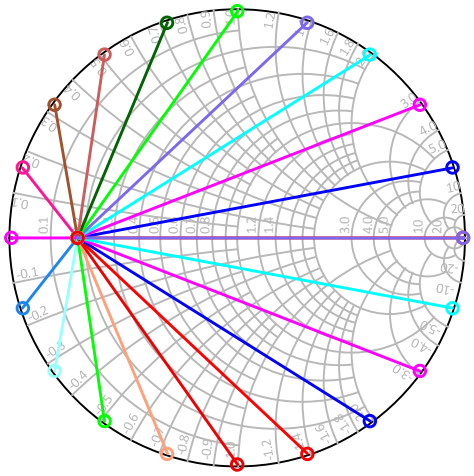

Figure 2.11: Swept 2nd Harmonic Termination with fixed Fundamental impedance at R_{opt}

This chocking reduces the magnitude of the fundamental component reducing the gain and efficiency. However, by overdriving the transistor recovering some of output power and efficiency is possible at the cost of linearity degradation. If entering the knee region can be remedied by modifying a certain parameter then it is possible to preserve the high efficiency performance of class B even when the second harmonic termination is not a short circuit anymore. Researchers found that by changing the

fundamental impedance it is possible to phase shift the voltage waveform such that the low voltage that used to push the device into the knee region coincides with a low current value to avoid sudden dip in current. A mathematical expression was derived to link the waveforms with the fundamental and second harmonic impedances and the design space concept was therefore conceived.

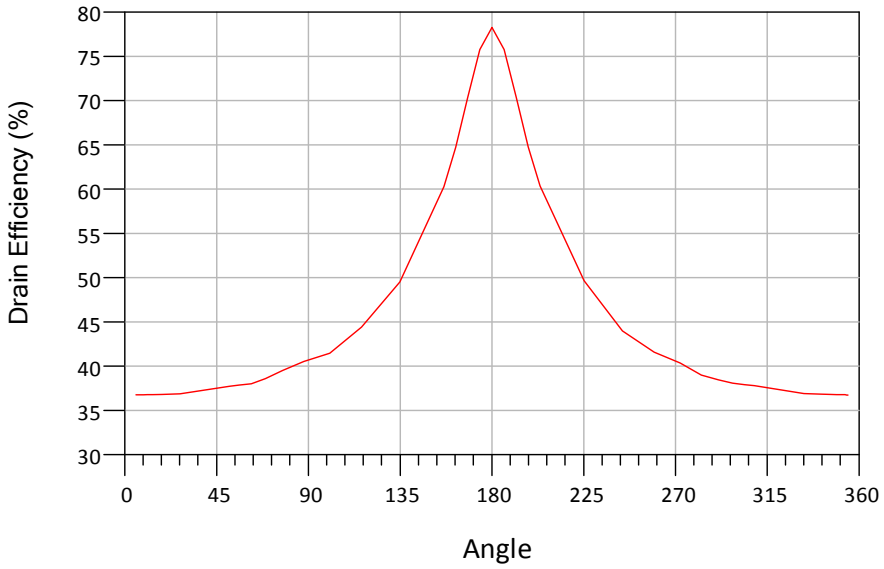

Figure 2.12: Drain Efficiency as a function of the angle of the 2nd harmonic termination

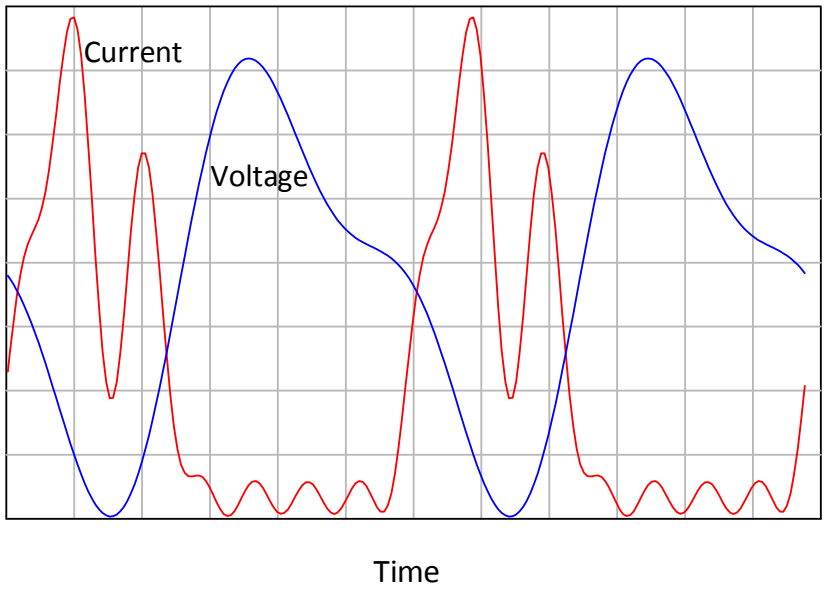

Figure 2.13: The voltage and current waveforms for class B power amplifier with a reactive 2nd harmonic termination

2.5.1.2 Design Space

It was shown in literature that a short circuit harmonic termination is not a unique solution for class B operation [3] and a new class of operation was introduced. The new class of operation presented the design space concept to expand the set of possible combinations under which the efficiency is maintained. This class of operation is referred to as class B/J. Class B/J, unlike other classes of operation, requires a complex fundamental load impedance and is not restricted to any specific load impedance for neither the fundamental nor the second harmonic. The current waveform for this class is always a half sine wave while the voltage waveform has the following expression,

$$V_{DS} = \overline{V_{DS}}(1 - \cos(\theta))(1 - \alpha \sin(\theta)) \qquad -1 \leq \alpha \leq 1 \tag{2.22}$$

The waveforms can be visualized for various values of α as shown in Figure 2.14. Note that class B operation occurs at $\alpha = 0$. The pairing between the fundamental and second harmonic terminations is shows in Figure 2.15.

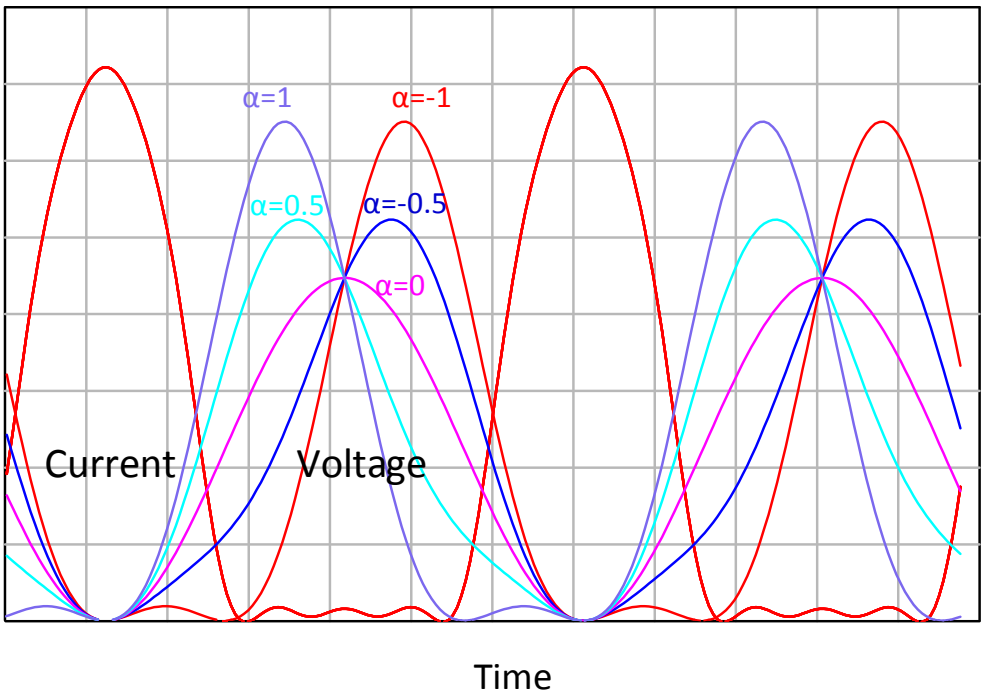

Figure 2.14: Current and Voltage waveforms for Class B/J operation for various values of α

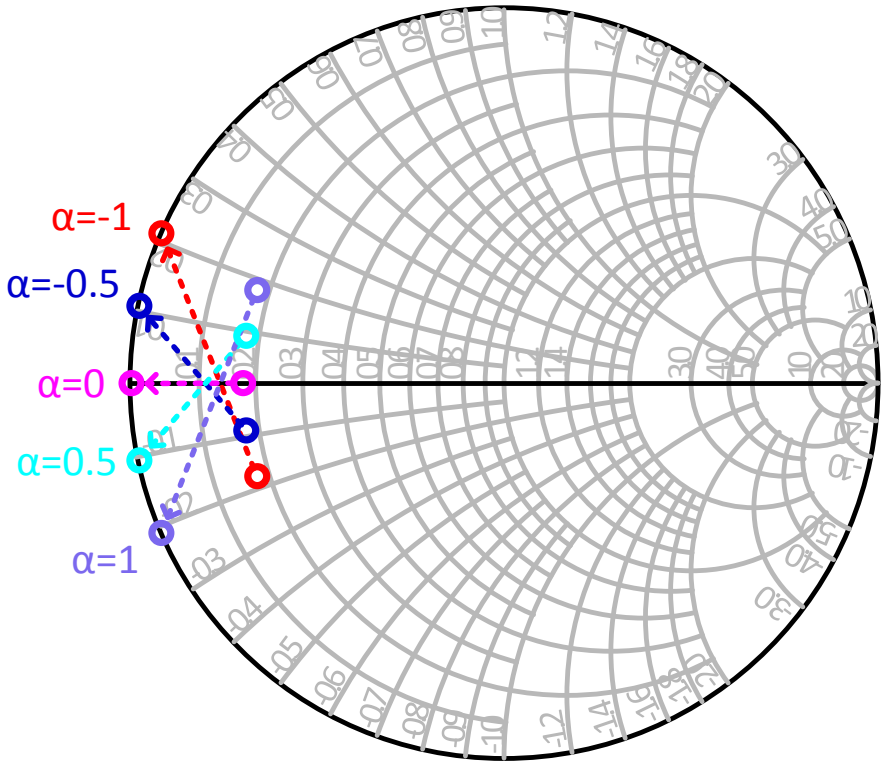

Figure 2.15: The pairing between fundamental and 2nd harmonic terminations for Ideal class B/J

One of the drawbacks of class B/J is the fact that the voltage can reach values as high as three times the bias voltage $\overline{V_{DS}}$ which makes this class of operation unsuitable for low breakdown voltage devices. The power and efficiency performance is identical to that of class B power amplifiers. The theoretical limitation of class B/J lay in having a maximum bandwidth of 50% when implemented according to the theory. Such limitation arises due to having to terminate the second harmonic at the edge of the smith chart with a reactive load rendering the frequencies unusable for real power transmission.

2.5.2 Push-Pull Topology

As explained earlier there is a theoretical bandwidth limitation on Class B/J power amplifiers. The Push-Pull topology does not have such limitation as it isolate the load termination of the second harmonic from that of the fundamental impedance. When implementing the Push-Pull topology along with class B/J it is theoretically possible to achieve high efficiency broadband designs that exceed the 50% bandwidth limitation and even penetrate to octave bandwidth. Figure 2.16 shows a simplified diagram for Push-Pull amplifier topology.

The main element in push-pull amplifiers is the antiphase power combiner which is also known as balanced to unbalanced (Balun) transformer. Baluns will be discussed in further details in the third chapter; however, there are several facts that must be pointed out in this section.

- High frequency Baluns behave differently than low frequency counterparts and most of the low frequency analysis does not apply to RF Baluns.
- Not all Baluns are the same even if they operate at the same frequency and have the same odd mode performance.
- Baluns can incorporate an impedance transformation ratio that can be used in the input and output matching circuits.

It is also worth noting that the input side of the power amplifier does not need a Balun and can be fed directly through a DAC. In fact it will be shown later that a Balun at the input might introduce some negative effect on the stability of the power amplifier depending on the Balun type and frequency of operation. The main purpose for the Balun is to isolate the fundamental impedance from the even mode harmonic impedances. Baluns have two modes of operation, Odd and even modes. When driving two transistors with antiphased signals the output's fundamental will be out of phase while the output's even order harmonics will be in phase with each other. When using a Balun as a power combiner then only the signals with opposite phases will be passed through to the load side while the in-phase counterparts will be rejected and terminated with a short, reactive or an open circuit load.

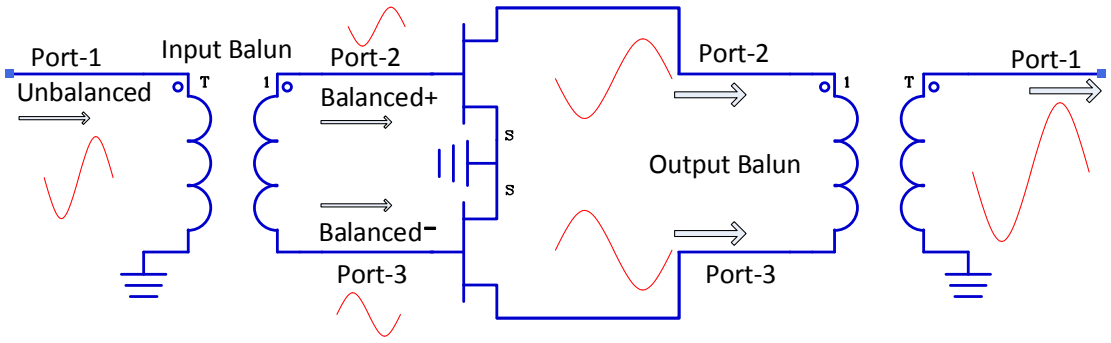

Figure 2.16: A simplified Push-Pull Power amplifier schematic

Chapter 3
Baluns

3.1 Introduction

This chapter will expand on the role of Baluns in Push-Pull amplifiers and how different topologies could affect the performance of the push-pull power amplifier. Firstly, a detailed Balun background will be presented introducing the ideal Balun and the three major Balun categories and elaborating on the difference between low frequency and high frequency Baluns. Then the most famous Balun topologies in literature will be introduced and critically analyzed in the context of balance, bandwidth and practicality. Finally, measurement results will be shown for several fabricated Balun prototypes.

3.2 Balun Theory

"[A] Balun is a network for the transformation from an unbalanced transmission line, system or device to a balanced line, system or device. Baluns are also used for impedance transformation. [The term Balun is] derived from balanced to unbalanced" [4]. Baluns are used as antenna feeds, inputs to differential circuits, Antiphase power combiners, transformers between transmission line types, etc. The definition of a Balun varies based on its use as it is more of a generic description that can take several forms in practice. For instance, an amplifier that takes a single ended input and outputs a differential signal can be referred to as an active Balun. This and other known structures such as the 180^{o} hybrid and a voltage transformer can be employed as passive Baluns.

3.2.1 Ideal Balun

The ideal Balun model is defined based on the application. As has been pointed out, a Balun can take several forms. In this thesis an ideal Balun will be thought of as an ideal three ports transformer as shown in Figure 3.1.

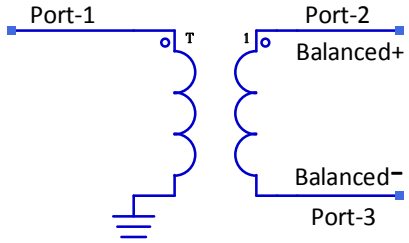

Figure 3.1: The ideal transformer employed as an ideal Balun

The Scattering matrix parameters (S-parameters) for the ideal transformer Balun are given by,

$$S = \begin{bmatrix} \frac{1-2T^2}{1+2T^2} & \frac{2T}{1+2T^2} & \frac{-2T}{1+2T^2} \\ \frac{2T}{1+2T^2} & \frac{1}{1+2T^2} & \frac{2T^2}{1+2T^2} \\ \frac{-2T}{1+2T^2} & \frac{2T^2}{1+2T^2} & \frac{1}{1+2T^2} \end{bmatrix}$$

For consistence during the analysis the transformation ratio T of the transformer for the ideal Balun model adopted in this work is,

$$T = \frac{1}{\sqrt{2}} \tag{3.1}$$

For this value of T the Balun will be matched at port 1 and the Balun will be acting as an antiphase power splitter for 50Ω reference impedance at all ports.

$$S = \begin{bmatrix} 0 & \frac{1}{\sqrt{2}} & \frac{-1}{\sqrt{2}} \\ \frac{1}{\sqrt{2}} & \frac{1}{2} & \frac{1}{2} \\ \frac{-1}{\sqrt{2}} & \frac{1}{2} & \frac{1}{2} \end{bmatrix}$$

According to microwave theory, it is impossible to have a lossless, matched and reciprocal three port device. Since the ideal Balun is lossless and reciprocal then it must be unmatched at all or some of the ports. It can be seen that ports 2&3 are unmatched and unisolated; however, under certain conditions these ports can behave as matched ports. To understand how a Balun operates we must look at two operating modes which are the odd and even modes of operation. Baluns act as an antiphase power combiner; hence, when operating in Odd-Mode the Balun combines the power coming from ports 2&3 and output them at port 1 Figure 3.2. In this case ports 2&3 appear to be matched since no power is reflected back from these terminals. The impedance seen by terminals 2&3 in this mode is given by (3.2) and is a function of the transformation ratio.

$$Z_{odd} = \frac{Z_o}{2T^2} = Z_o \tag{3.2}$$

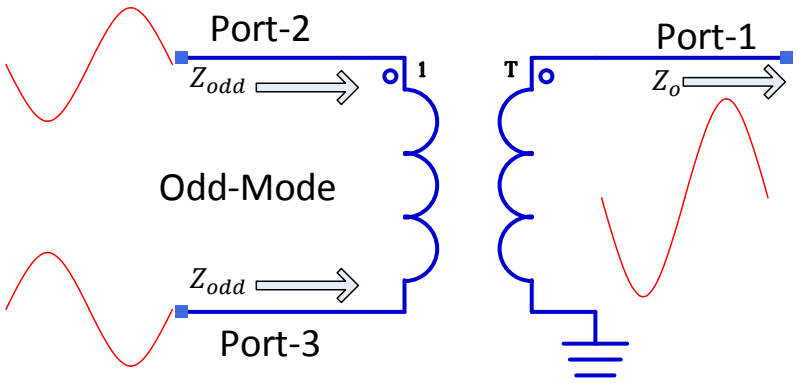

Figure 3.2: Odd-mode behavior of an ideal transformer-based Balun

When the Balun is operating under Even-mode conditions, the power is completely reflected from ports 2&3 and the impedance seen at these ports is an open circuit.

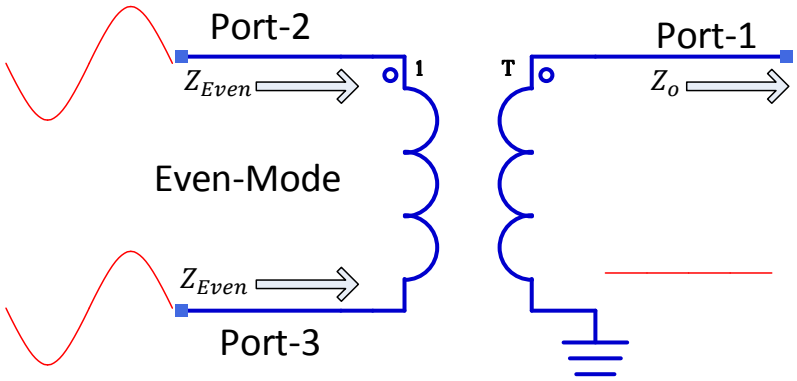

Figure 3.3: Even-mode behavior of an ideal transformer-based Balun

A more general formulation which describes the reflection coefficient at the balanced ports in each mode when the unbalanced port is terminated by the characteristic impedance Z_o is given by,

$$S_{Odd} = \frac{1}{2}\big(S(2,2) - S(2,3) - S(3,2) + S(3,3)\big) \tag{3.3}$$

$$S_{Even} = \frac{1}{2}\big(S(2,2) + S(2,3) + S(3,2) + S(3,3)\big) \tag{3.4}$$

3.2.2 Balun Categories

Not all Baluns are identical in function and they can be categorized into three main categories namely, current Baluns, Voltage Baluns and Baluns not belonging to either categories [5].

3.2.2.1 Current Baluns

Baluns belonging to this category are characterized by always having a balanced current at the two output terminals regardless of the loads terminating ports 2&3. The famous example of this type of Balun is the ideal transformer shown in Figure 3.1. Other examples of current Baluns are the low frequency Guanella and coaxial Marchand.

3.2.2.2 Voltage Baluns

Similarly a voltage Balun maintains balanced voltages at both terminals irrespective of the loads connected there. A famous example of this type of Baluns is the ideal transformer with the secondary winding grounded in the center as shown in Figure 3.4.

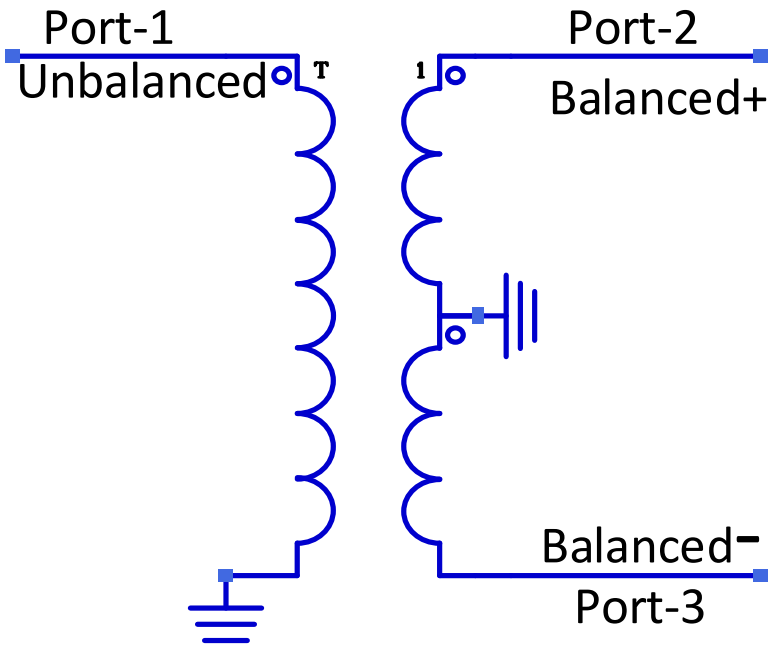

Figure 3.4: Ideal voltage Balun based on transformer with grounded center tap

3.2.2.3 180^o Power Dividers

Some references named the third category as 180^o Power Dividers as Baluns belonging to this category "fix a linear combination of voltage and current at the two output ports to be equal in magnitude and opposite in phase" [5]. An example of this type is the 180^o hybrid with its isolation port terminated with a matched load Figure 3.5.

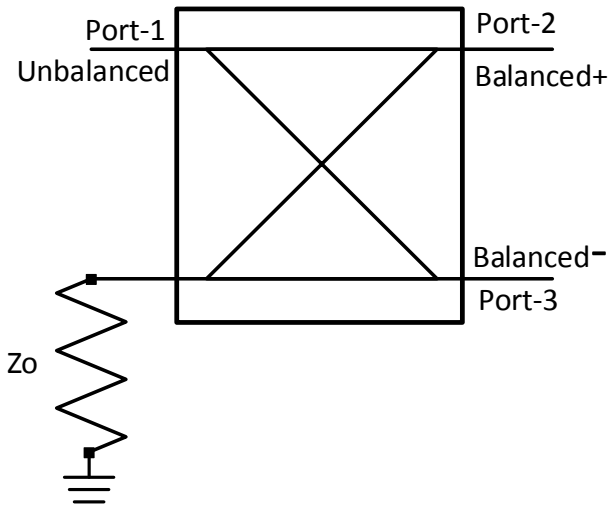

Figure 3.5: A 180^o hybrid employed as Balun with the use of matched load at the isolated port

In this thesis most of the focus will be on this category as it was found that at RF frequencies Baluns can be voltage Baluns at one frequency and current Baluns at another while at most of the other frequencies its behavior falls under the third category.

3.2.3 Major RF Balun Topologies

3.2.3.1 Bridge (Lattice, Star or Y) Balun

The bridge Balun is among the simplest practical high frequency Baluns to design and is considered an all-Pass Balun when connected to a differential load as shown in Figure 3.6. The impedance seen at the input under the condition that both input and load impedances have equal real parts is given by,

$$Z_{in} = \frac{(X_C - X_L)^2 R_L}{(4R_L^2 + (X_C + X_L)^2)} = R_{in} \tag{3.5}$$

In order for the input impedance R_{in} to equal the load impedance R_L the value of C and L should be set such that,

$$R_{in} = R_L = \sqrt{X_C X_L} = \sqrt{L/C} \tag{3.6}$$

However, when used as an antiphase power splitter and combiner as shown in Figure 3.7 then it only operates at a single frequency defined by resonance frequency f_{res} of the LC network,

$$f_{res} = \frac{1}{2\pi\sqrt{LC}} \tag{3.7}$$

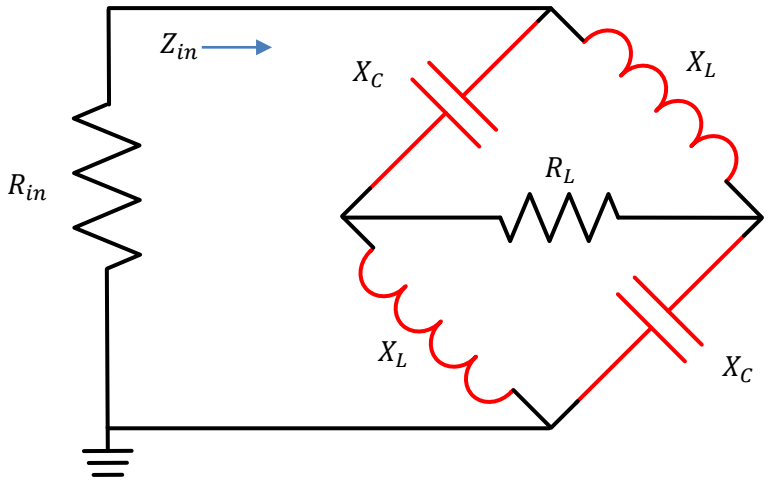

Figure 3.6: LC lattice Balun employed as transmission line transformer in its All-Pass form

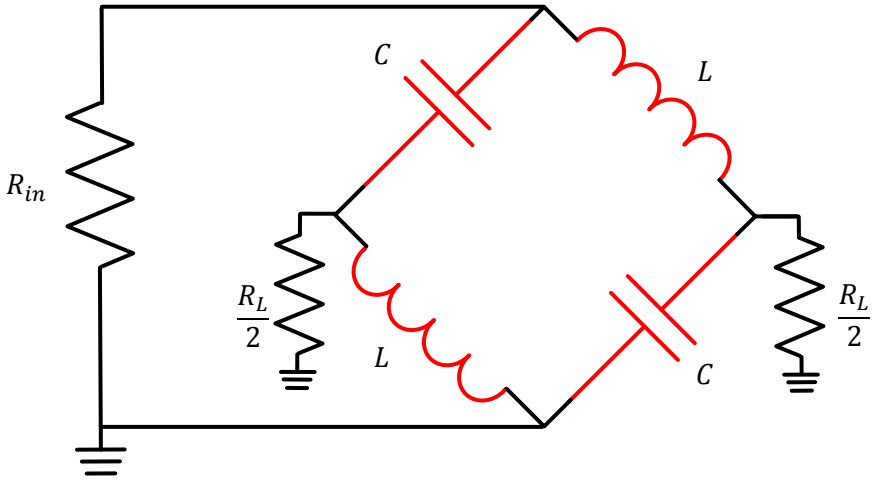

Figure 3.7: LC lattice Balun used as an Antiphase power splitter and combiner

This topology can be used for narrow band Push-Pull amplifiers [6]; however, a broader band or a dual band variation can be synthesized using higher order LC networks in place of the reactive elements [7] [8] and [9]. Other variations also exist using distributed transmission lines as reactive elements with the help of the Richard transformation [10] and another is using Coplanar Waveguides (CPW) as presented in [11].

3.2.3.2 180 ^{o} Hybrid Couplers

It was illustrated earlier how a coupler can be used as an antiphase power splitter behaving as a Balun in some applications. Several researchers have reported this concept in literature and implemented Baluns using modified 4-port networks terminated with a short, open or matched load at the unused port [12] and [13]. It is important to note that terminating with a short or a matched load results in a different behavior and one should be aware of the difference in certain applications. To elaborate we need to recall the fact that three port networks cannot be matched, lossless, and reciprocal all at the same time. The Rat-Race hybrid coupler shown in Figure 3.8 will be used as an example; it has the following s-parameters,

$$S = \frac{-j}{\sqrt{2}}\begin{bmatrix} 0 & 1 & 0 & -1 \\ 1 & 0 & 1 & 0 \\ 0 & 1 & 0 & 1 \\ -1 & 0 & 1 & 0 \end{bmatrix}$$

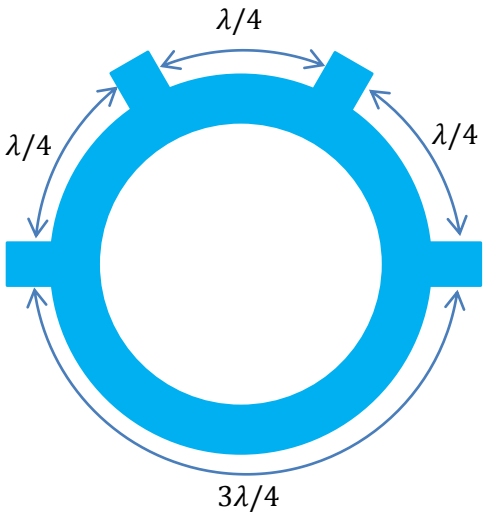

Figure 3.8: The Rat-Race hybrid coupler

From the s-parameters we can deduce that if power is incident on port 1 then ports 2&4 produce antiphase signals while port 3 is considered isolated from port 1 as it receives nothing. If we chose to terminate port 3 with a matched load then the result will be a three port device that acts as an antiphase power splitter with all ports matched and reciprocal.

$$S = \frac{-j}{\sqrt{2}}\begin{bmatrix} 0 & 1 & -1 \\ 1 & 0 & 0 \\ -1 & 0 & 0 \end{bmatrix}$$

According to microwave theory the resultant 3-port network cannot be lossless and this shows when we have two signals in phase incident at ports 2&4 (even mode). In this scenario the input power is completely dissipated in the matched load at port 3 and there will be no output power at any of the ports. The fact that ports 2&4 are isolated when port 3 is matched caused this response. Such a configuration is not suitable to be used at the output of push-pull amplifiers operating under class B/J since the second harmonic is incident at ports 2&4 in phase and will be absorbed and dissipated into the matched load at port 3 reducing the efficiency of the amplifier.

If the matched load at port 3 was replaced with a short circuit then the network will stay lossless and reciprocal; however, it will not remain matched anymore and will have the following S-parameters,

$$S = \frac{-j}{\sqrt{2}}\begin{bmatrix} 0 & 1 & -1 \\ 1 & \frac{j}{\sqrt{2}} & \frac{j}{\sqrt{2}} \\ -1 & \frac{j}{\sqrt{2}} & \frac{j}{\sqrt{2}} \end{bmatrix}$$

The difference between the isolated Balun and non-isolated lay mainly in the even mode behavior. In fact, the odd mode in both cases (matched and shorted) is identical. The even mode in this configuration is presented with an open circuit just like an ideal transformer Balun this conclusion can be reached using (3.4). Similarly, when terminating port 3 in the rat-race coupler with an open circuit the even mode impedance becomes a short circuit instead. We need to note that having bad isolation in Baluns has its perks in some applications especially in Push-Pull amplifiers which operate under class B/J.

3.2.3.3 Guanella

The Guanella Balun was first reported in 1944 in a paper titled “New Method of Impedance Matching in Radio-Frequency Circuits” [14]. The Guanella Balun has several forms. The ideal Guanella is presented with an ideal transformer connected as shown in Figure 3.9. The Guanella is high pass by nature but is limited in practice by the maximum frequency the transformer can handle. The RF variation of Guanella can be modeled as a coupled line instead of the transformer Figure 3.10.

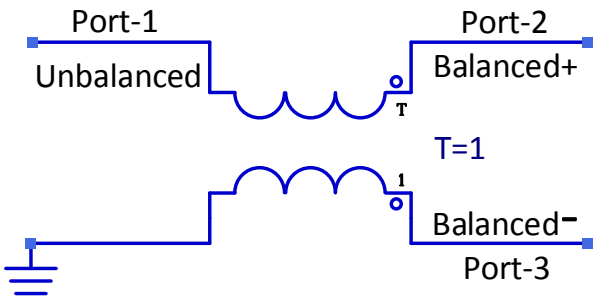

Figure 3.9: The ideal Guanella model based on the ideal transformer

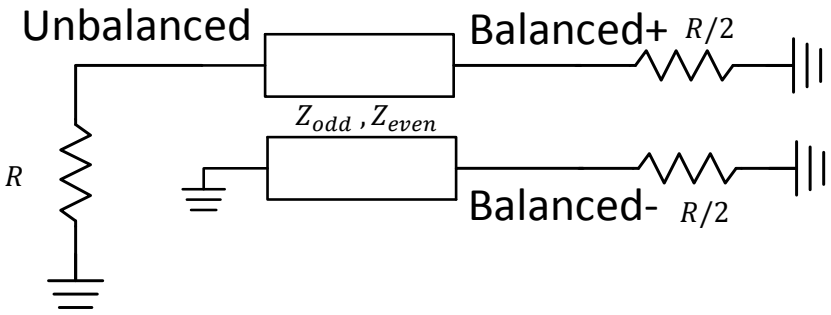

Figure 3.10: The ideal Guanella model based on the coupled line model

The ideal high frequency distributed element Guanella equivalent is a coupled line with a unity coupling coefficient (C). The transformation ratio of this topology is always 1:1 and the odd impedance of the coupler is equal to half the source and load impedances $Z_{odd} = R/2$. The even mode impedance needs to be as high as possible to increase the coupling coefficient. In practice, unity coupling coefficient is unrealizable; however, high coupling coefficients are possible but depends on the fabrication process and the design to be implemented. The coupling coefficient dictates the balance between the balanced ports. The higher the coupling coefficient of the Balun the better the balance. The balance is defined by two measures namely the magnitude imbalance and the phase imbalance. For a coupling coefficient of

$$C = \frac{Z_{even} - Z_{odd}}{Z_{even} + Z_{odd}} = \frac{200 - 25}{200 + 25} = 0.7778 \tag{3.8}$$

It is possible to have the following Guanella Balun performance Figure 3.11

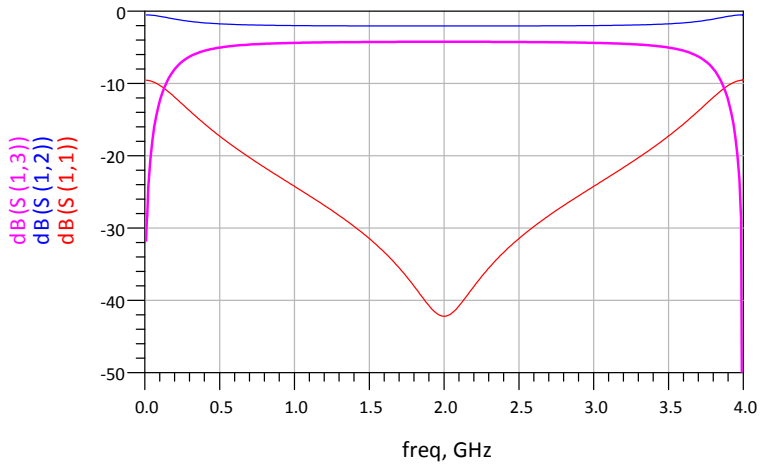

Figure 3.11: An illustration of the Guanella Balun performance when the coupled line has a coupling coefficient of 0.7778

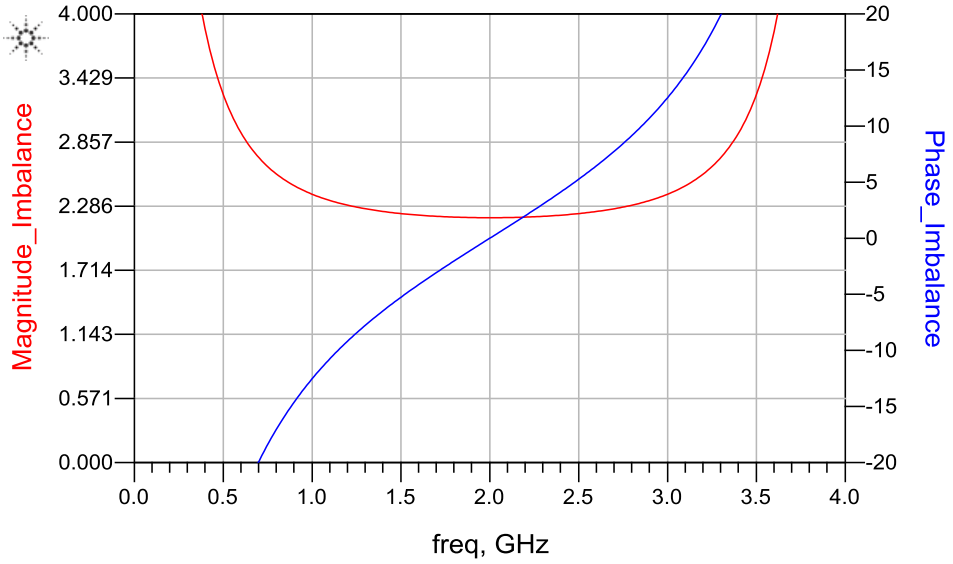

Figure 3.12: An illustration of the Guanella Balun Balance performance when the coupled line has a coupling coefficient of 0.7778

Figure 3.13 shows the relation between the magnitude imbalance and coupling coefficient.

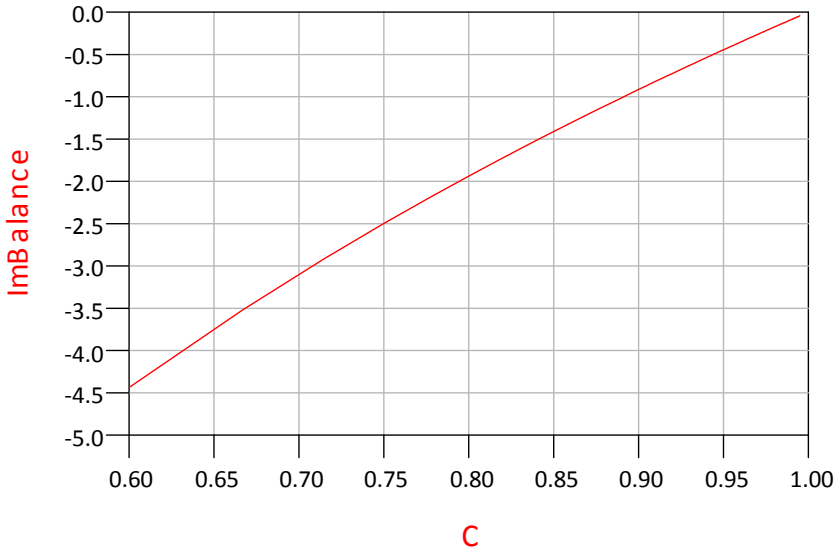

Figure 3.13: The relation between the magnitude imbalance and coupling coefficient C

This Balun goes under bandpass characteristics when using distributed elements due to the periodicity of the Richard domain [10] and [15]. However, this type of Baluns has a better return loss bandwidth compared to Marchand Balun. The Guanella has a fixed transformation ratio per order of topology. Using more couplers increases the topology order hence increasing the transformation ratio between source and load impedances [16].

3.2.3.3.1 Ruthroff variation

Ruthroff [17] published an alternative variation with compensation short circuit stub to improve the balance from the original Guanella. To demonstrate, Figure shows the performance of a Guanella Balun constructed with a coupling coefficient of $C = 0.8824$.

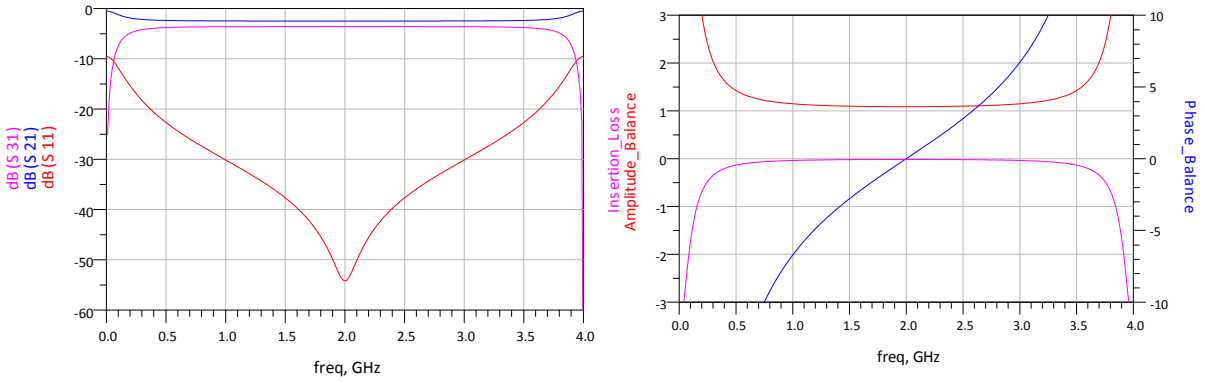

Figure 3.14: The performance of a Guanella Balun using a coupled line with $C = 0.8824$

The proposed Ruthroff variation is shown in Figure which includes a short circuit stub with an impedance equal to the average of Z_{even} & Z_{odd}.

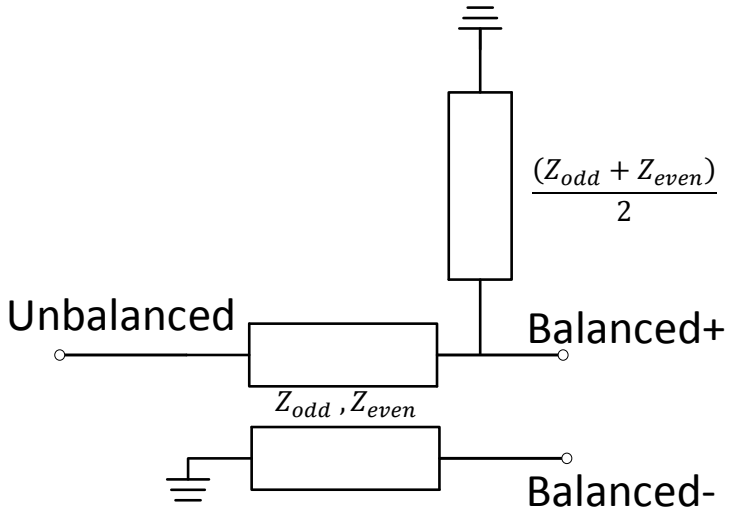

Figure 3.15: Ruthroff Variation of the Guanella Balun with $C = 0.8824$ with added short circuit stub

The stub improves the phase balance over the entire bandwidth and makes the magnitude imbalance consistent over all frequencies as shown in Figure 3.16.

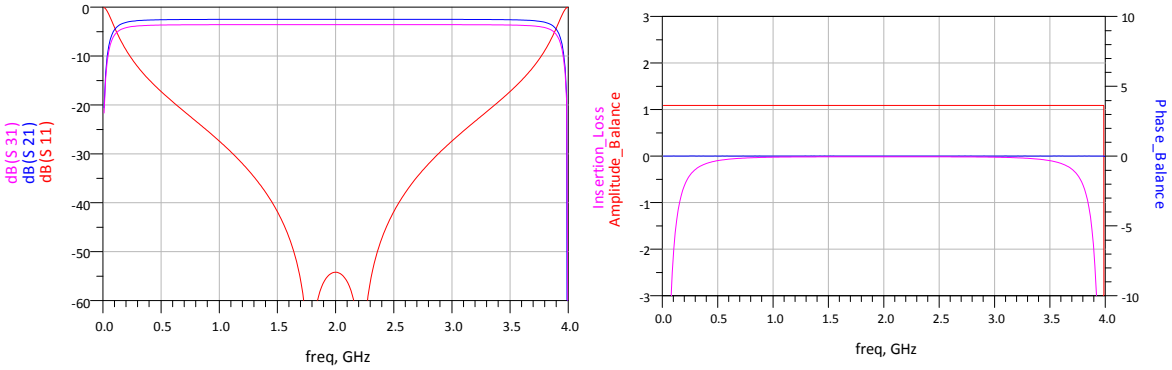

Figure 3.16: The performance of the Ruthroff variation with improved balance

This topology has surfaced again recently in several publications [18] and [19] as it provided broadband behavior and good balance.

3.2.3.4 Marchand

The Marchand Balun was introduced in a paper titled “Transmission-line conversion transformers” by N. Marchand in 1944 [20]. The original concept was developed using coaxial cables as shown in Figure 3.17.

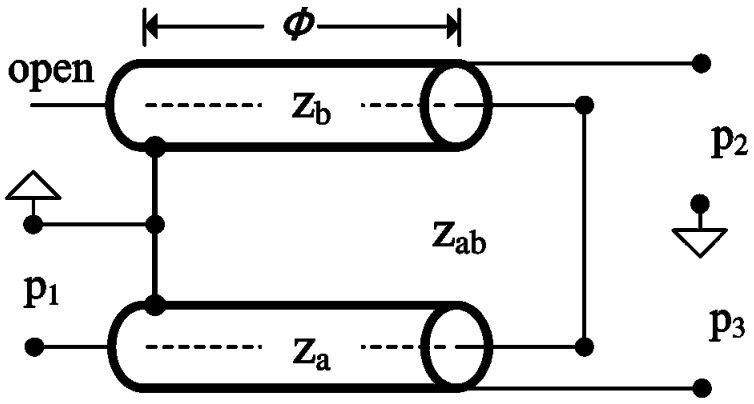

Figure 3.17: Coaxial representation of the Marchand Balun [18]

This Balun has superior balance performance compared to other Baluns but it has a bandpass characteristics and its return-loss bandwidth is inferior to that of the Guanella Balun. The Marchand Balun has a well-established theory and it can achieve various transformation ratios between the source and load impedances without the need for more elements. The Marchand Balun can be implemented in planner form using couplers instead of coaxial cable sections as shown in Figure 3.18. The couplers can be defined using any two out of four parameters namely the odd mode impedance (Z_{odd}), the even mode impedance (Z_{even}), the characteristic impedance (Z_o), and the coupling coefficient (C). For perfect balance these coupled lines need to be identical even if they are asymmetric. However, using identical couplers limits the maximum bandwidth achievable for a certain impedance transformation ratio. It is possible to use non identical couplers to obtain wider bandwidth for the same impedance transformation ratio; however, that will be at the expense of the balance of the Balun.

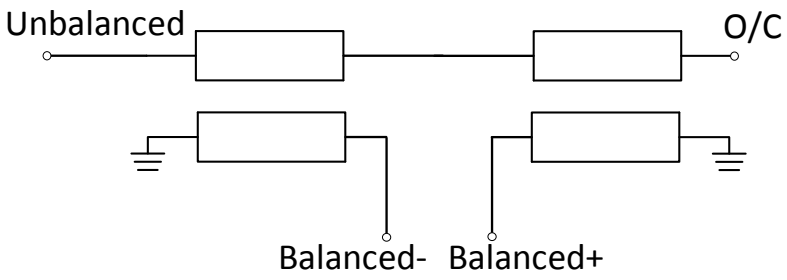

Figure 3.18: The planner equivalent of Marchand Balun using two coupled lines

When the couplers are of the same length and coupling coefficient $C_1 = C_2$, the Marchand Balun can be viewed as a bandpass filter using three elements as shown in Figure 3.19. When both couplers are $\lambda/2$ in length then each element in the filter equivalent topology is also $\lambda/2$ in length and their values can be computed from the couplers' parameters as follows [21],

$$Z_1 = Z_{o_1}\sqrt{(1 - C_1^2)} \tag{3.9}$$

$$Z_2 = Z_{o_2}\sqrt{(1 - C_2^2)} \tag{3.10}$$

$$Z_3 = \frac{Z_{o_1}C_1^2}{\sqrt{(1 - C_1^2)}} + \frac{Z_{o_2}C_2^2}{\sqrt{(1 - C_2^2)}} \tag{3.11}$$

Where Z_o is the characteristic impedance, the subscript 1 denotes the coupler connected to the unbalanced port and the subscript 2 denotes the coupler connected to the open circuit termination. The balanced port impedance should be scaled by a factor of C^2 in order for it to be used in the filter representation accurately. There are several papers that did a study on numerical solutions for Marchand Balun in terms of bandwidth and return loss requirements [21] and [22]. These references however didn't point out that the balance will be jeopardized under certain conditions such as when the Balun is used as an antiphase power splitter.

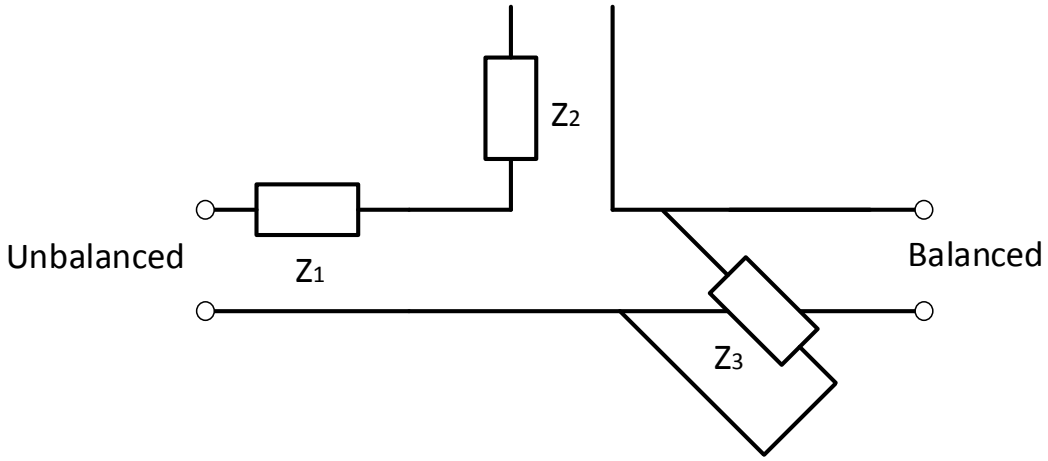

Figure 3.19: The three elements band-pass filter equivalent of the Marchand Balun

From this equivalent structure Figure 3.19 we can compute S_{11} accurately but predicting the magnitude of S_{21} & S_{31} is not guaranteed except when using identical couplers then $Z_1 = Z_2$ and the magnitude of S_{21} & S_{31} is exactly 3dB less than the transmission coefficient of the filter equivalent. As for the case where the couplers are not identical then there will be imbalance in the two branches.

The even mode; however, is modeled differently and is much simpler as it is composed of one element Figure 3.20. Note that the balanced port should have the modified scaling factor C^2 in order for the model to be accurate. If the application does not require a reactive even mode behavior then it is possible to provide a broadband matched load instead by adding an even mode matching network to the output of the Balun [23]. Further increase in bandwidth can achieved using topologies with multiple stages [24].

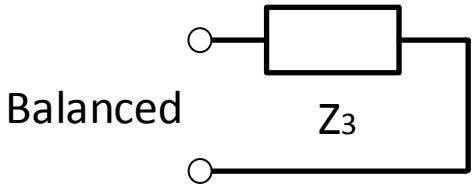

Figure 3.20: The even mode equivalent circuit of the Marchand topology

3.2.3.4.1 Marchand Balun in Push-Pull Power Amplifiers

The Marchand Balun can be described in two separate modes of operation (even and odd) as explained earlier. If the Balun is balanced then the equations for odd and even modes can be used to

compute the impedances the power amplifier is seeing. These equation are given again here for convenience,

$$S_{Odd} = \frac{1}{2}\big(S(2,2) - S(2,3) - S(3,2) + S(3,3)\big) \tag{3.12}$$

$$S_{Even} = \frac{1}{2}\big(S(2,2) + S(2,3) + S(3,2) + S(3,3)\big) \tag{3.13}$$

In order to test the theory, a simulation testbench was used to compare a single ended power amplifier with a Push-Pull power amplifier providing similar odd and even mode impedances. Equations (3.12) and (3.13) were used to compute the even and odd impedances presented by an arbitrary Marchand Balun design which was employed in a Push-Pull Amplifier design as shown in Figure 3.21. These impedances were then used to terminate a single ended power amplifier biased in Class B Figure 3.22. The source in the push-pull topology had twice the input power and twice the source impedance in order to match its performance to that of the single ended topology. The resulting waveform comparison given in Figure 3.23 which compares the voltage waveforms after the DC-Block at the drain side shows that both topologies are operating with the same performance and mode of operation.

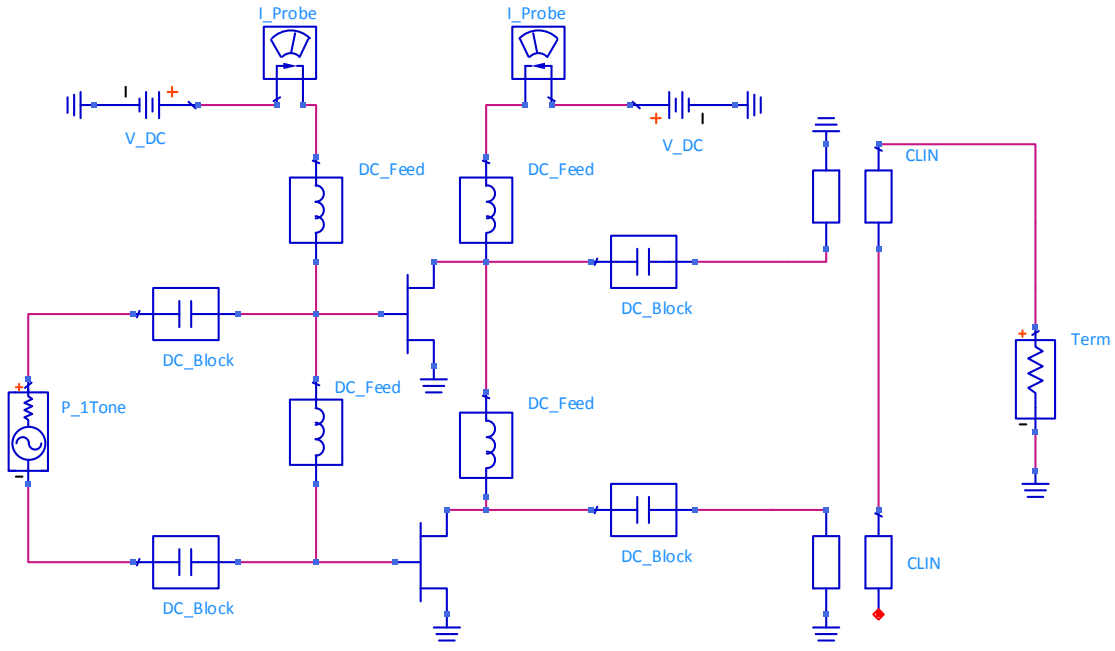

Figure 3.21: Push-Pull amplifier schematic using Marchand Balun with ideal couplers

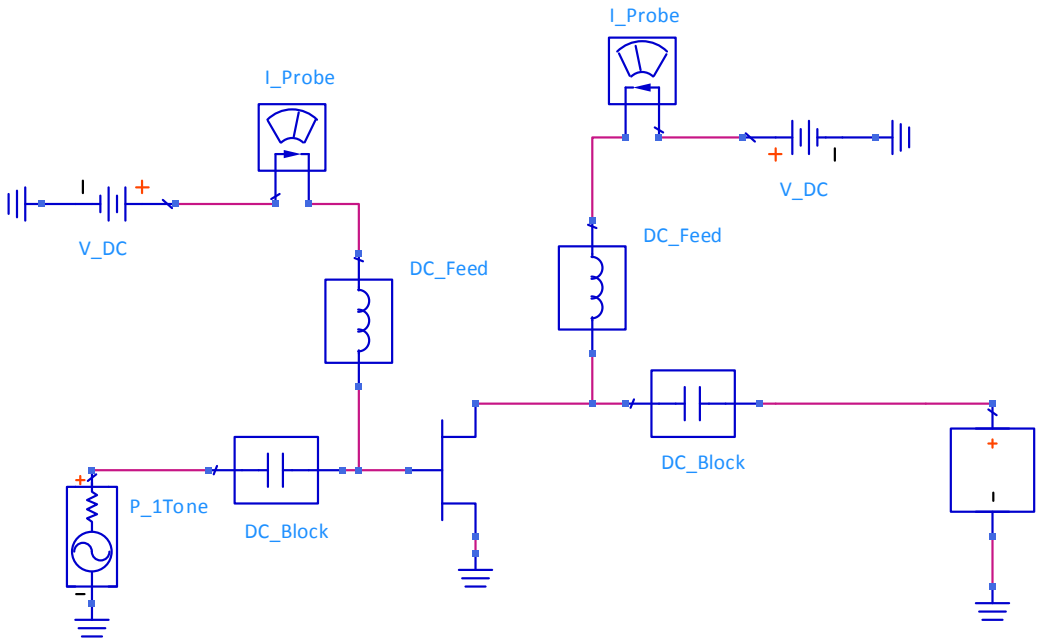

Figure 3.22: Single ended equivalent power amplifier schematic for comparison with Push-Pull power amplifier

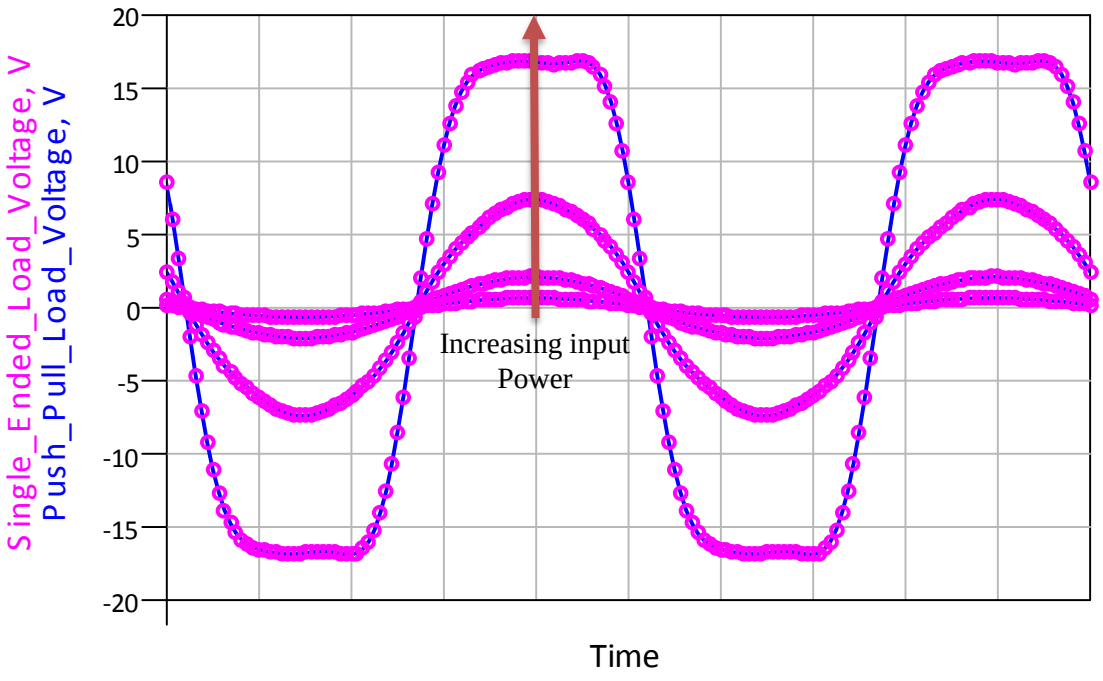

Figure 3.23: Voltage waveform comparison between the two schematic proving the equivalency

3.3 Baluns Design

In order to examine the operation of the Guanella and Marchand topologies, several prototype Baluns were implemented with a transformation ratio of 1:1. The specifications targeted were as follows.

Table 3.1: The targeted specifications for the fabricated Balun prototypes

Specification	Target
Frequency range	$1GHz - 3GHz$
Magnitude Imbalance	$\pm 0.2\ dB$
Phase Imbalance	$\pm\ 3^{o}$
Load impedance for output ports $\boldsymbol{R_L/2}$	$50/2\ \Omega$

For the design of high coupling coefficient couplers, we referred to ground patterning and coplanar waveguides with patterned ground plane [19], [18] and [25]. The resulting couplers are asymmetric with high coupling coefficient when used properly. The designs were made using High Frequency Structural Simulator (HFSS) from Ansys and Advanced Design System (ADS) from Agilent. One of the final fabricated boards is shown in Figure 3.24.

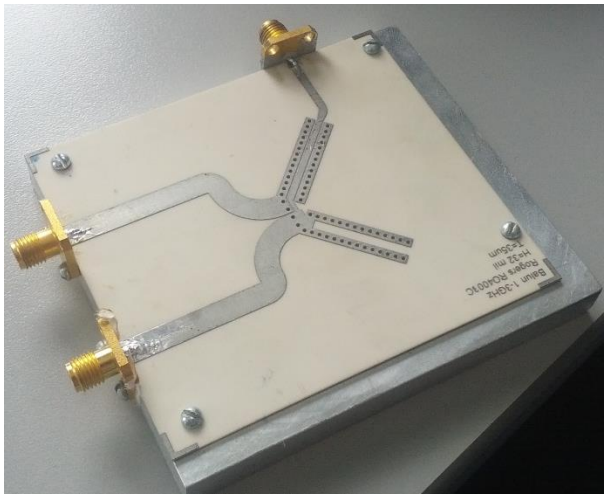

Figure 3.24: The fabricated Guanella-based Ruthroff variation Balun (prototype 1)

Two of the prototypes where designed based on the Guanella topology implementing the Ruthroff variation. One of these two prototypes was designed with an even-mode matching network. The remaining three prototypes where based on the Marchand topology. The ideal design assumed ideal coupled lines which can't be implemented in practice due non-idealities. The fabricated coupled lines

where asymmetric and had a frequency behavior that is dispersive and difficult to model using ideal components.

The measurement results were obtained using “Agilent PNA-X Network Analyzer” as shown in Figure 3.25, Figure 3.26,

Figure 3.27, Figure 3.28 and Figure 3.29.

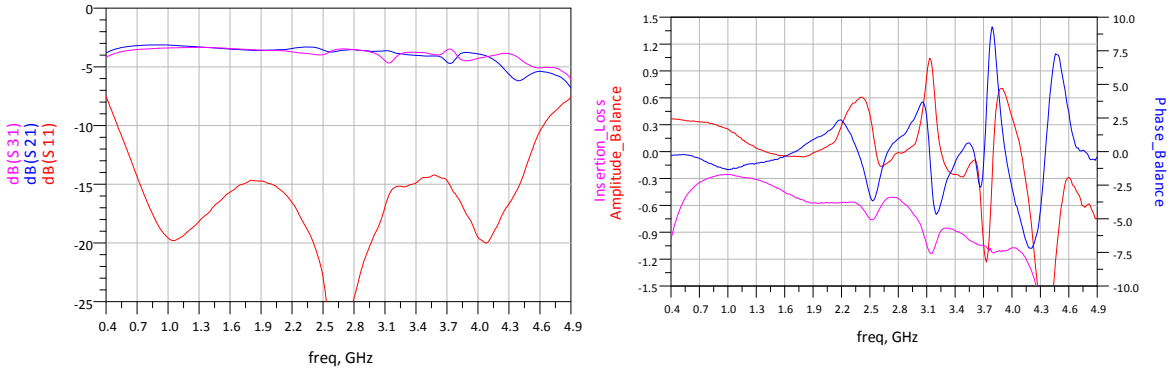

Figure 3.25: Guanella-based Ruthroff variation Balun performance of prototype 1

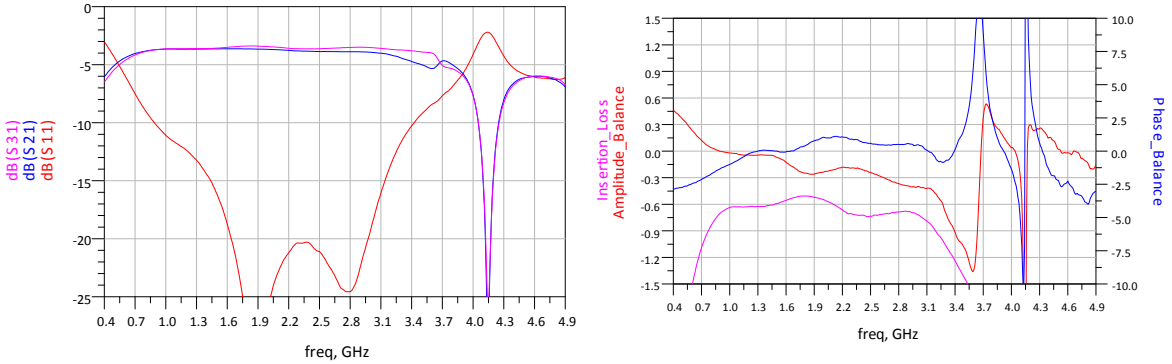

Figure 3.26: Guanella-based Ruthroff variation Balun performance of prototype 2

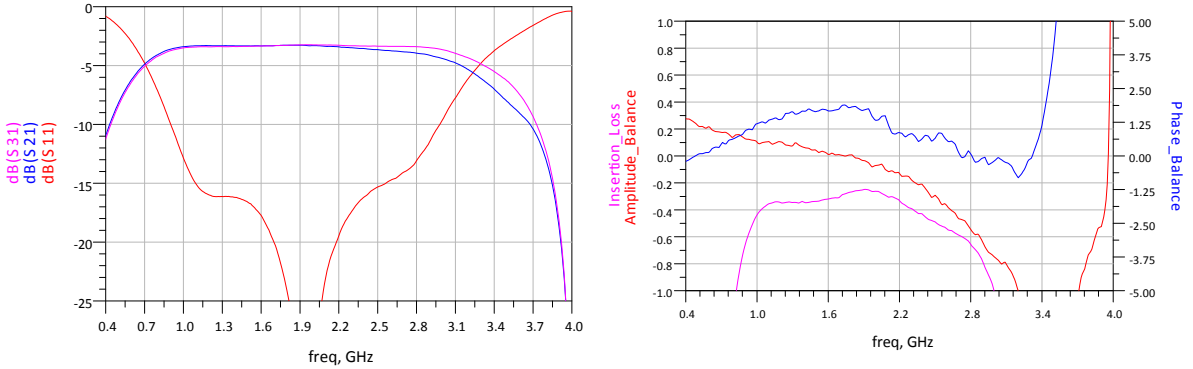

Figure 3.27: Planner Marchand Balun performance of prototype 3

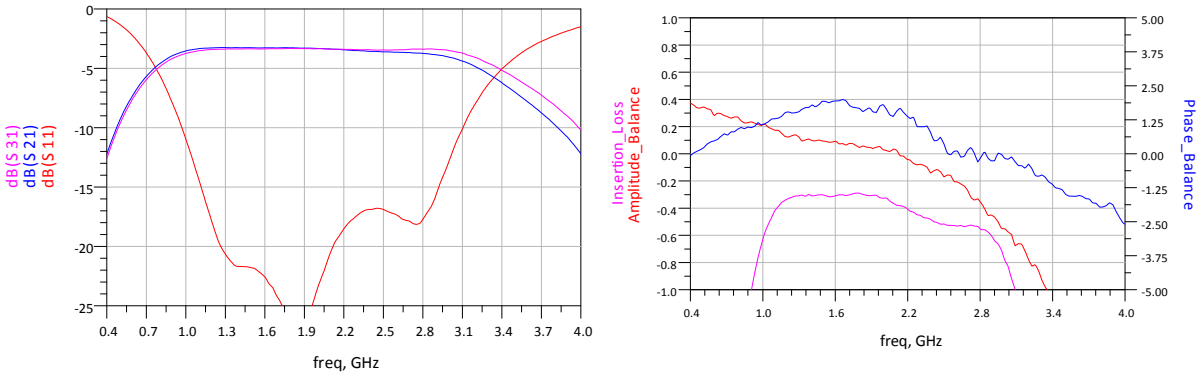

Figure 3.28: Planner Marchand Balun performance of prototype 4

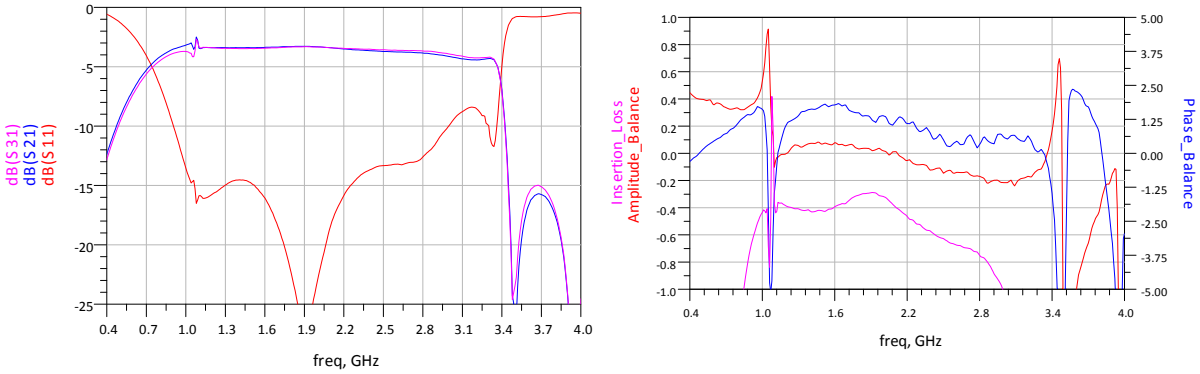

Figure 3.29: Planner Marchand Balun performance of prototype 5

After investigating the previous topologies in actual implementation it was found that both Guanella and Marchand topologies offer bandwidths higher than 50% which means both can offer bandwidth that exceed the theoretical limitations of class B/J. It was also found that the Guanella topology and its variations have the best bandwidth at the expense of balance. The Marchand topology has relatively better balance than the Guanella due to its inherent symmetry; however, this balance is not guaranteed in practice due to dispersion and parasitics.

Chapter 4
Push-Pull Design and Simulation

4.1 Introduction

This chapter will present the design procedure and simulation results of this work. Firstly, the push-pull power amplifier design steps will be presented and the design choices will be explained and justified. Then the LTCC technology will be introduced and its advantages for our application. The design abstracted layouts and procedure will be illustrated and finally the simulation results of the whole design will be shown and criticized.

4.2 Push-Pull Power Amplifier Design

The targeted specification were derived from Table 1.1 based on targeted frequency bands, power level, Peek to Average Power Ratio (PAPR), and number of simultaneous connections. The targeted frequency bands are between 0.7GHz to 2.7GHz and the maximum power level was chosen to be 60 Watts. The design will be using two 30 Watts Cree GaN HEMT DIEs (CGH60030D) in push-pull configuration.

4.2.1 Load Pull Results

A single transistor Figure 4.1 was used to determine the optimum load and source impedances to be targeted when we design the Baluns. The transistors will be biased at class B with $V_{DS} = 28V$ & $V_{GS} = -3.1V \rightarrow \overline{I_{DS}} = 70mA$. From load pull characterization, it was found that an impedance value of 15Ω is suitable over the targeted range of frequencies from 0.7-3GHz. The drain efficiency was found to be above 70% and the gain is between 20-10dB as shown in Figure 4.2.

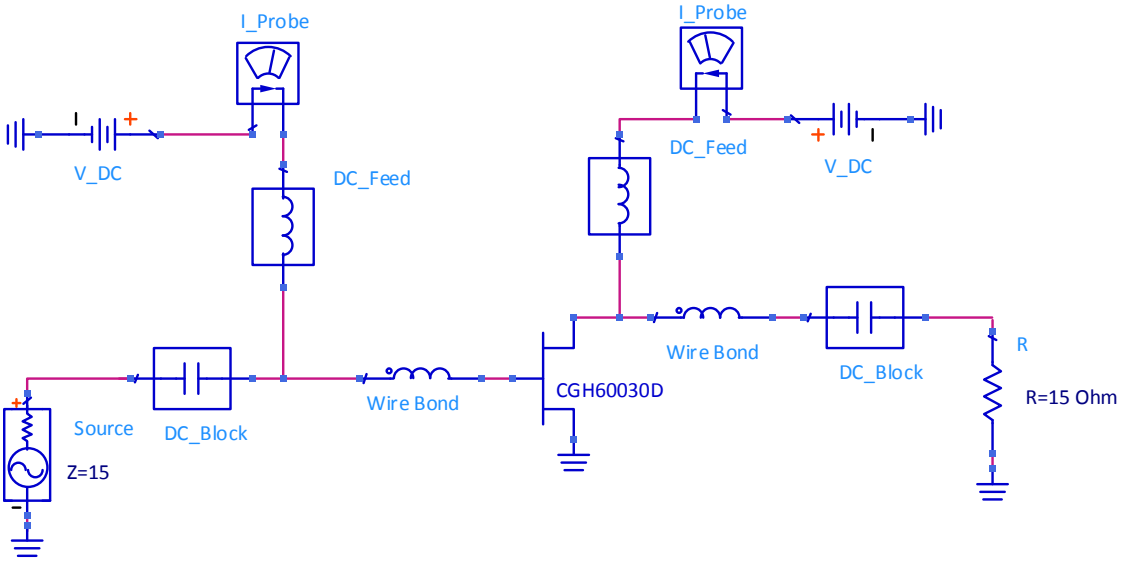

Figure 4.1: Single ended load-pull schematic setup used to determine fundamental impedances

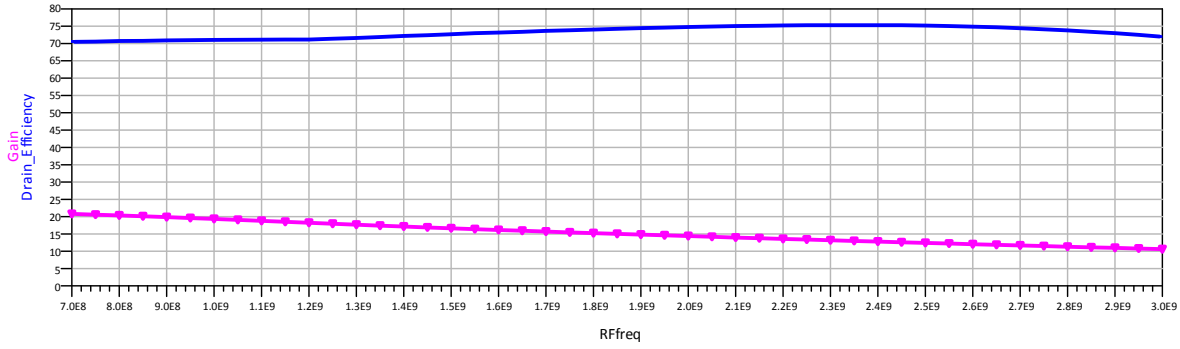

Figure 4.2: preliminary performance with impedance terminations of 15Ω at both Source and Load

4.2.2 LTCC Baluns

LTCC stands for Low Temperature Co-fired Ceramics, a multilayered ceramic technology which is designed for high frequency applications. It has several advantages over standard PCB technology. The advantages are as follows:

- Supports various types of transmission lines and impedances.
- Low loss and high dielectric constant substrate.
- Allows the use of surface mount components and custom DIEs.
- Withstands high temperatures up to 350^{o}C.

- Operates at high frequencies $> 30GHz$.
- Highly customizable layer thicknesses and material selection from the vendor.

The LTCC process used in the design was provided by IMST in Germany through CMC Microsystems and it had 6 ceramic layers and 7 metal layers Figure 4.3.

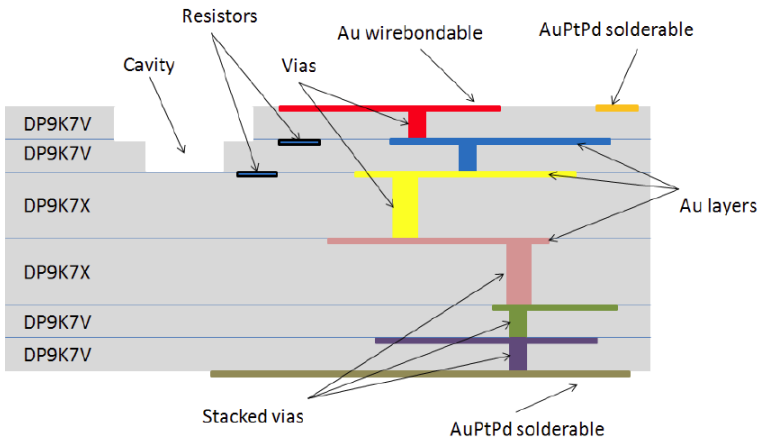

Figure 4.3: A cross section of the LTCC process layers showing the metal layers and relative thickness of the ceramic layers [26]

For this design, it was decided to pursue the Marchand Balun topology for two main reasons. Firstly, to the best of the author's knowledge this topology has not been implemented in RF Push-Pull amplifiers before. Secondly, this topology has inherent AC coupling between the input and output ports which helps in avoiding the use of a series capacitor to decouple the DC biasing from the RF source. The use of a series capacitor could limit the bandwidth of operation due to parasitics that causes self-resonance. Two Identical Marchand Baluns with transformation ratio of 1:2 were designed for both input and output stages of the Push-Pull Amplifier Figure 4.4. The Baluns were matched to 15Ω at all ports using metal layers two and three which have a spacing of $121\mu m$ between them. The small spacing is useful for designing couplers with sufficiently high coupling coefficient and low characteristic impedances.

The biasing feed for this design was done in a novel way which, according to the author's knowledge, was not done before in RF Push-Pull power amplifiers in the targeted range of frequencies. Figure 4.5 shows a schematic of where the biasing feed will be located. The points where the Baluns were connected to ground were used for biasing along with capacitors to provide the RF short circuit to ground.

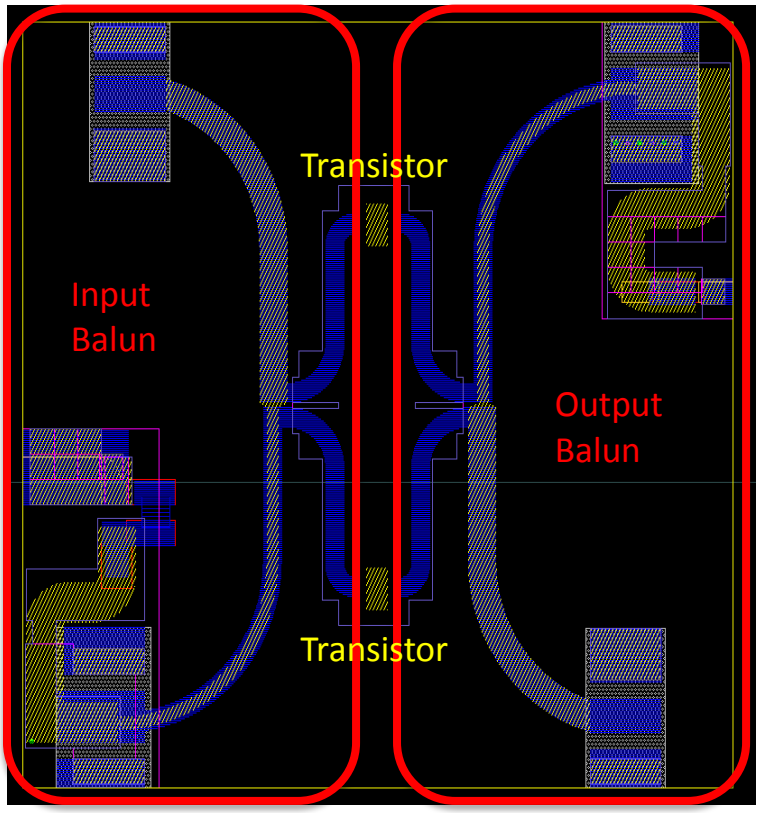

Figure 4.4: The abstracted LTCC layout showing the overall design of both input and output Baluns

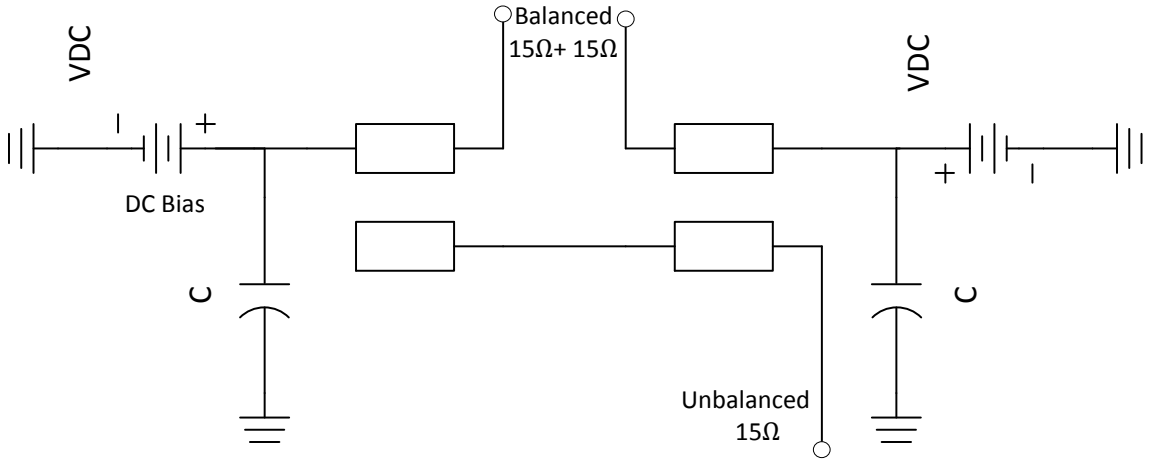

Figure 4.5: The schematic diagram of the designed Baluns

The fabricated LTCC prototype without the transistor DIEs is shown in Figure 4.6. The transistors were placed on top of metal three which is connected to the ground plate through gold filled vias for

thermal dissipation and electrical grounding. Figure 4.7 shows the 30 Watts Cree DIE placed using silver epoxy and wire-bonded to one of the balanced terminals of each Balun.

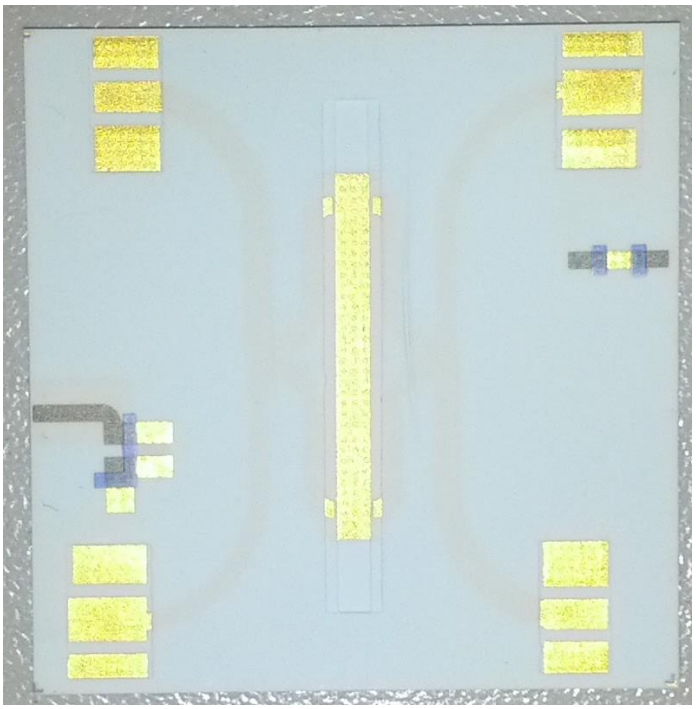

Figure 4.6: The fabricated LTCC prototype without the transistor DIEs

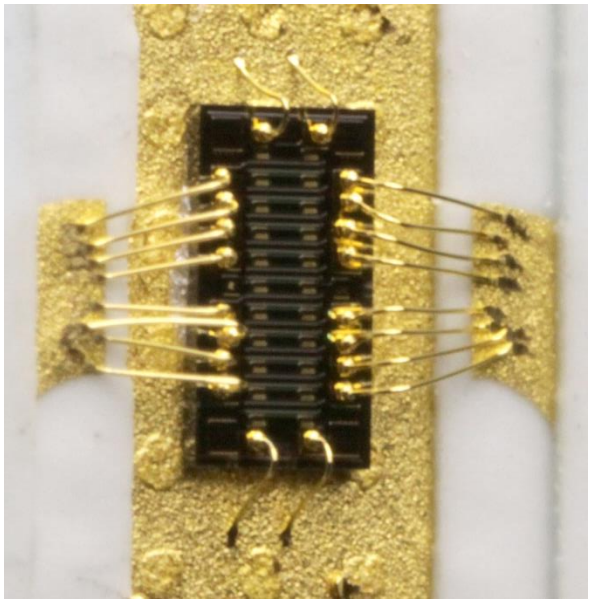

Figure 4.7: A Photo of the wire-bonded 30 W Cree DIE

4.2.3 External Matching Networks

The Balun is the element that dictates the even order harmonic terminations in Push-Pull power amplifier topologies. Therefore, after finalizing the Balun design, the 2nd harmonic terminations were essentially fixed while the odd order harmonics are still affected by the impedance seen at the unbalanced port of the Baluns. Hence, it is possible to tune the fundamental impedance independently from the 2nd harmonic termination. This concept was conceived while observing the load and source pull results after the inclusion of the Balun in the design. Instead of terminating the port with a 15Ω impedance it was found that other terminations will lead to marginal improvement. This was attributed to the fact that class J/B requires a different fundamental impedance for every 2nd harmonic termination presented to the transistor.

Two matching networks were designed to tune the fundamental impedance for a better pairing with the 2nd harmonic termination presented by the Balun. The design criteria was to optimize both the gain and efficiency. The matching networks were designed using ADS software on Rogers RO4003C substrates with thickness of $810\mu m$ and metal thickness of $35\mu m$. Figure 4.8 shows the location of the external matching networks.

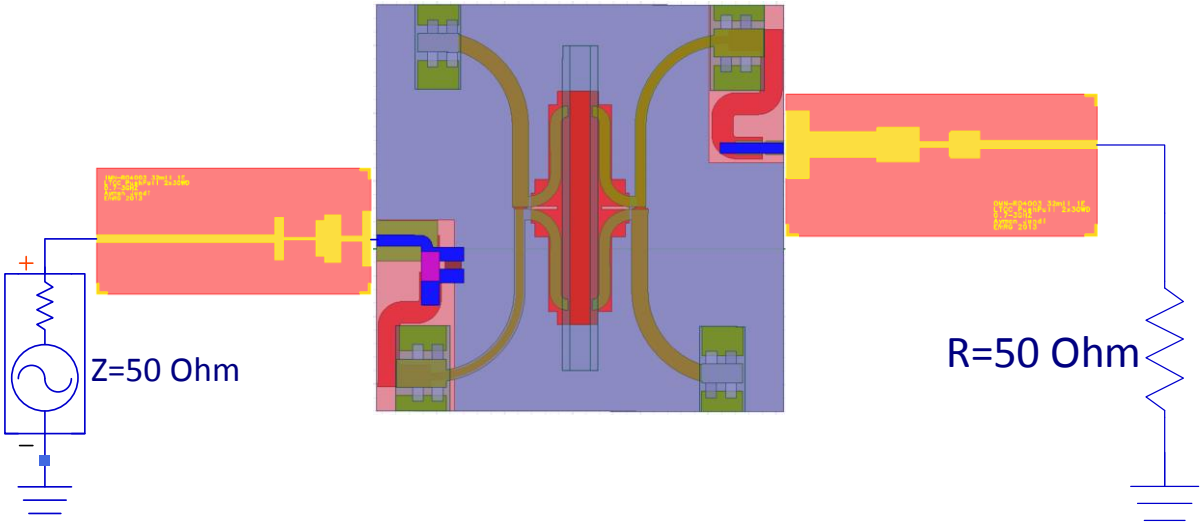

Figure 4.8: The complete Push-Pull power amplifier design showing the location of the external matching networks

4.3 Simulation Results

4.3.1 LTCC Baluns Simulations

The complete LTCC structure was simulated using HFSS. Figure 4.9 shows the final LTCC layout as it was sent for manufacturing. The location of all surface mount components, transistor DIEs, and input and output ports were all placed on the layout amounting to a total of 23 ports. The breakdown of the ports is as follows, 3 ports per Balun for ports, 1 port for stabilization network, and 16 ports for RF grounding capacitors connected at the DC bias pad.

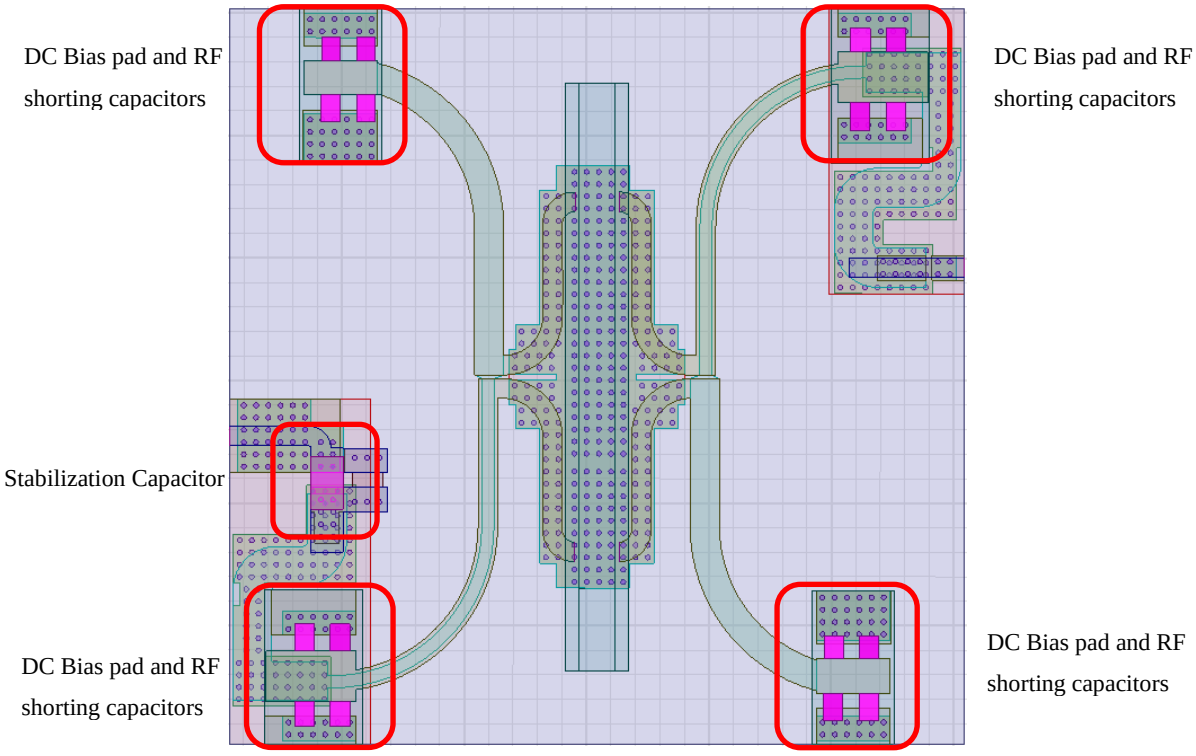

Figure 4.9: The complete layout of the fabricated LTCC simulated using HFSS showing the various ports in the network

The s-parameters of the 23 ports network was computed for the frequency range from 0.1GHz to 12GHz covering the 4th harmonic of the highest frequency. The results were saved and taken into ADS to determine suitable capacitor values. The S-parameters of the matching networks and bond wires were then incorporated into the network and the resulting odd mode and even mode's S-parameters are shown in Figure 4.10 covering the frequency range from 0.7GHz to 3.0GHz.

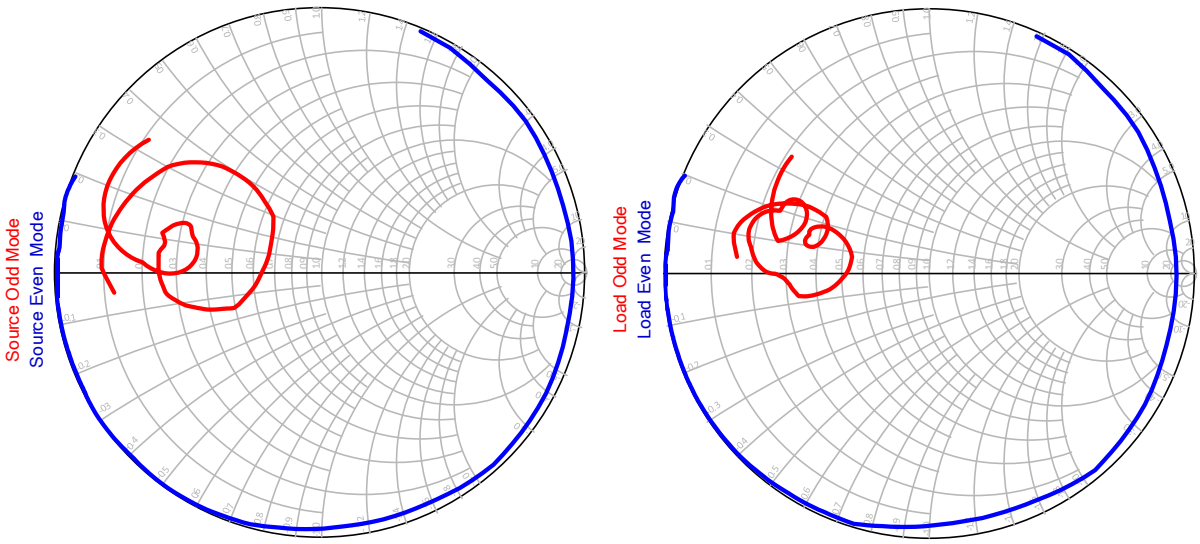

Figure 4.10: Source and Load odd and even mode impedances as a function of frequency from 0.7GHz to 3GHz

4.3.2 Push-Pull Power Amplifier Simulation Results

The power amplifier schematic was put together and simulated using ADS. In order to test if the Balun is suppressing the 2nd order harmonic power from passing through to the load, the power was measured for all the harmonics at the 50Ω output port. Figure 4.11 shows the harmonic power content in dBm measured at the load at 800MHz.

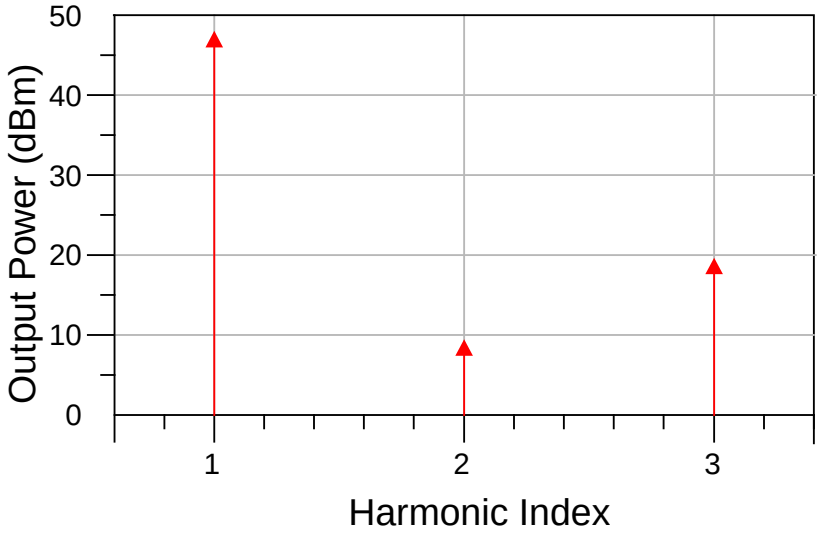

Figure 4.11: Harmonic power content from the push-pull power amplifier at the load side at 800MHz

It can be seen that the 2nd harmonic power is 38.5 dBc which corresponds to a satisfactory rejection ratio significantly reducing the requirements of the multiplexing stage following the power amplifier. The rejection ratio was measured for the remaining frequencies and the result is shown in Figure 4.12.

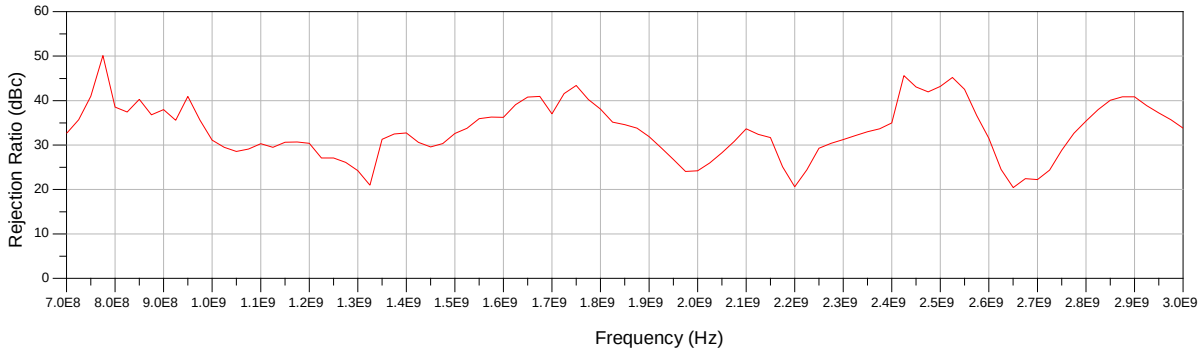

Figure 4.12: The ratio of the 2nd harmonic power to the fundamental power in dBc over the frequency range 0.7GHz-3GHz

The performance results obtained from the simulation were promising over the bands of interest. Bandwidth (0.7GHz-2.9GHz) , 45%< Drain Efficiency<75% in the bands of interest, 10dB≤ Gain ≤ 25dB and 46dBm < Output power < 48.4dBm. The results are shown in Figure 4.13. The drop in performance between 1.3GHz and 1.4GHz can be attributed to a possible second harmonic termination being in a low efficiency region [27]. It is also possible to be attributed to the second harmonic termination at the source side as well. This will be investigated further in the future after the actual measurements have been completed. The corresponding 100MHz band (from 1.3GHz-1.4GHz) does not contain any of the targeted frequencies bands for mobile communication.

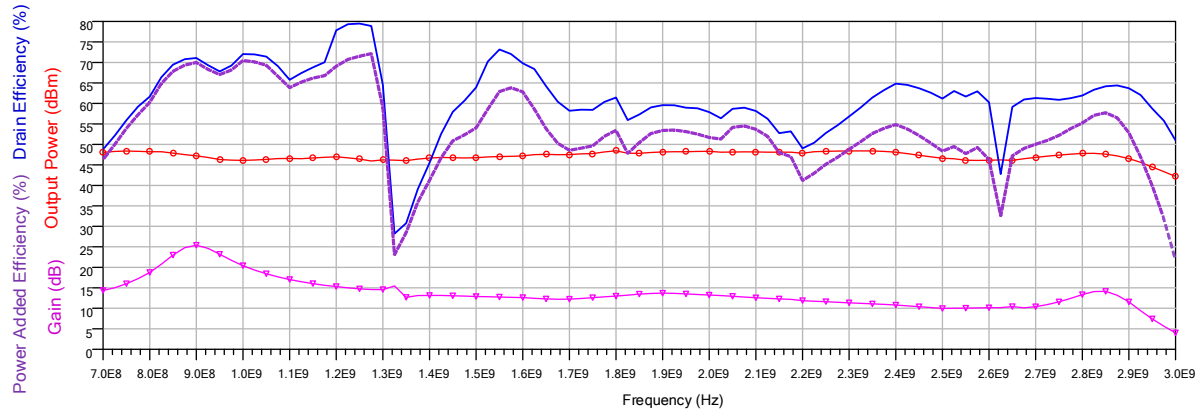

Figure 4.13: The final simulation results of the completed Push-Pull power amplifier

A comparison was made with previous designs existing in literature and the results were tabulated in Table 4.1. Given the fact that the drop in efficiency happened outside the targeted bands it will not be considered in our results. However, in future designs such degradation in performance will be addressed in the design stage to avoid a similar scenario.

Table 4.1: Comparison table between this work and other existing works in literature

Ref	Frequency (MHz)	BW (%)	P_{out} (dBm)	PAE (%)	Gain (dB)
[28]	250-3100	170	40-46	16-65	7-20
[27]	1400-3400	84	38-41	50-62	7-10 (LS)
[19]	500-2500	133	41-43	47-63	16-18
This work	700-2900	122	46-48.5	40-72*	10-25 (SS)

* This is only valid over the bands of interest

- SS: Small Signal , LS: Large Signal

Chapter 5
Conclusion and Future work

5.1 Conclusion

This work was mainly motivated by the need for multimode multiband (MMMB) transmitters. It was shown how communication protocols occupy many frequencies and use many different standards. The potential application in communication gateways targeting intelligent transportation systems services is a driving factor in developing true MMMB transmitters. It was demonstrated how a broadband power amplifier is the key foundation for any potential development in high efficiency MMMB power amplifiers.

Various power amplifier topologies were investigated and analyzed in terms of performance. A comparison was established with the classical well known class A power amplifier topology. Some high efficiency single ended power amplifier classes were introduced and noted to be useful for narrow band applications; however, they cannot be used as they are for bandwidths greater than 50%. Push-Pull power amplifier topology was then introduced and found to have the greatest potential in providing high efficiency performance with broadband performance surpassing that of any single ended topology.

It was shown that the Balun is the major element in dictating the proper operation of a Push-Pull amplifier topology. The ideal Balun was defined in the context of our application and illustrated using ideal components. The differences between low frequency and high frequency Baluns were explained to clarify the challenges facing an RF designer; various Balun topologies were also presented pointing out their advantages and disadvantages in the context of push-pull power amplifier design. Several prototypes were manufactured and tested to verify the theory and design tools.

The design methodology of the design push-pull power amplifier was presented. Load and source pull results are important in providing a useful insight on the potential of the transistors being used in the design. From load and source pull results, the fundamental load and source impedances were set. The advantages of LTCC technology were then listed and the design of the Baluns was carried out. A novel way of connecting the bias feed was introduced to the design of the Balun; this biasing technique simplified the complexity of the design close to the transistor. The rejection of the second harmonic was demonstrated over the bandwidth and the performance of the overall push-pull power amplifier was presented. It was noted that there was a dip in efficiency in the frequency range from

1.3GHz to 1.4GHz which was attributed to the second harmonic terminations presented at the source and load sides. So far the cause have not been isolated exactly and it is unclear if the main contributor is the source side or the load side. Preliminary testing did point to the source but the load side is also a contributor; therefore, further investigation will be made when fabrication and assembly are completed.

5.2 Future work

There is still a lot of work to be done to improve the theory of Balun design. The theory of the Marchand Balun presented using coupled lines is only valid when the couplers are symmetric; however, coupled lines structures used in practice are usually asymmetric in order to satisfy the high coupling coefficient requirement to obtain a wide bandwidth. The asymmetry of the coupled line causes inconsistent coupling and the dispersive behavior will vary depending on the way the coupler is connected; this asymmetry needs to be properly modeled for a more comprehensive involvement of the theory in the design stage.

The effect of the second harmonic termination on the load side is well established; however, due to the presence of parasitics and nonlinear elements it is sometimes difficult to account for the deviation from theory. Moreover, it was shown earlier that the second harmonic termination at the load side has a significant effect on the waveform which will affect the gain and linearity most of all. The second harmonic termination at the source side was not investigated thoroughly in this work and is to be done when practical measurements are completed.

Wider bandwidths were demonstrated in literature using Baluns based on the Guanella topology. The main advantage of using the Marchand Balun is the inherent balance; however, if the modeling for asymmetric couplers with high coupling coefficient is completed, then it is possible to implement a broadband Guanella Balun with excellent balance suitable for push-pull power amplifier topologies. Moreover, wider bandwidth guarantees better rejection of the second harmonic over a wider range of frequencies since there is no guarantee of balance outside the operation range. Finally, a more systematic design approach will be devised.

Bibliography

[1] K. Golestan, A. Jundi, L. Nassar, F. Sattar, F. Karray, M. Kamel and S. Boumaiza, "Vehicular Ad-hoc Networks(VANETs): Capabilities, Challenges in Information Gathering and Data Fusion," in *Autonomous and Intelligent Systems*, M. Kamel, F. Karray and H. Hagras, Eds., Springer Berlin Heidelberg, 2012, pp. 34-41.

[2] S. Cripps, RF power amplifiers for wireless communications, second edition, Artech House, Incorporated, 2006.

[3] S. Cripps, P. Tasker, A. Clarke, J. Lees and J. Benedikt, "On the Continuity of High Efficiency Modes in Linear RF Power Amplifiers," *Microwave and Wireless Components Letters, IEEE,* vol. 19, no. 10, pp. 665-667, 2009.

[4] P. Laplante, Comprehensive Dictionary of Electrical Engineering, Second Edition, Taylor \& Francis, 2005.

[5] J. McLean, "Balancing networks for symmetric antennas .I. Classification and fundamental operation," *Electromagnetic Compatibility, IEEE Transactions on,* vol. 44, no. 4, pp. 503-514, 2002.

[6] W. Bakalski, W. Simburger, H. Knapp, H. D. Wohlmuth and A. Scholtz, "Lumped and distributed lattice-type LC-baluns," in *Microwave Symposium Digest, 2002 IEEE MTT-S International*, 2002.

[7] D. Kuylenstierna and P. Linner, "Design of broadband lumped element baluns," in *Microwave Symposium Digest, 2004 IEEE MTT-S International*, 2004.

[8] D. Kuylenstierna and P. Linner, "Is the second order lattice balun a good solution in MMICs - a comparison with a direct-coupled transformer balun," in *Microwave Symposium Digest, 2005 IEEE MTT-S International*, 2005.

[9] D. Kuylenstierna and P. Linner, "Design of broad-band lumped-element baluns with inherent impedance transformation," *Microwave Theory and Techniques, IEEE Transactions on,* vol. 52, no. 12, pp. 2739-2745, 2004.

[10] J. Walker, Classic Works in RF Engineering: Combiners, Couplers, Transformers, and Magnetic Materials, Artech House on Demand, 2006.

[11] V. Trifunovic and B. Jokanovic, "Four decade bandwidth uniplanar balun," *Electronics Letters*, vol. 28, no. 6, pp. 534-535, 1992.

[12] F. Burdin, F. Podevin, A. L. Franc, E. Pistono, D. Gloria and P. Ferrari, "Miniaturized low-loss millimeter-wave rat-race balun in a CMOS 28 nm technology," in *Microwave Workshop Series on Millimeter Wave Integration Technologies (IMWS), 2011 IEEE MTT-S International*, 2011.

[13] C. Inui, Y. Manzawa and M. Fujishima, "On-Chip S-Shaped Rat-Race Balun for Millimeter-Wave Band Using Wafer-Level Chip-Size Package Process," in *Microwave Integrated Circuit Conference, 2008. EuMIC 2008. European*, 2008.

[14] G. Guanella, "New method of impedance matching in radio-frequency circuits," *The Brown Boveri Review*, vol. 31, pp. 327-329, 1944.

[15] B. Yarman, Design of Ultra Wideband Power Transfer Networks, Wiley, 2010.

[16] A. Grebennikov, "Power combiners, impedance transformers and directional couplers," *High Frequency Electronics*, vol. 6, no. 12, pp. 20-38, 2007.

[17] C. Ruthroff, "Some Broad-Band Transformers," *Proceedings of the IRE,* vol. 47, no. 8, pp. 1337-1342, 1959.

[18] Z. Xu and L. MacEachern, "Optimum Design of Wideband Compensated and Uncompensated Marchand Baluns With Step Transformers," *Microwave Theory and Techniques, IEEE Transactions on,* vol. 57, no. 8, pp. 2064-2071, 2009.

[19] Y.-P. H. S. S. K. M. P. M. A. Jonmei J. Yan, "Broadband High PAE GaN Push-Pull Power Amplifier for 500MHz to 2.5 GHz Operation," in *Microwave Symposium Digest (MTT), 2013 IEEE MTT-S International*, 2013.

[20] N. Marchand, "Transmission-line conversion transformers," *Electron,* vol. 17, pp. 142-146, 1944.

[21] C. L. Goldsmith, A. Kikel and N. L. Wilkens, "Synthesis of Marchand baluns using multilayer microstrip structures," *International Journal of Microwave and Millimeter-Wave Computer-Aided Engineering*, vol. 2, no. 3, pp. 179-188, 1992.

[22] J. H. Cloete, "Exact Design of the Marchand Balun," in *Microwave Conference, 1979. 9th European*, 1979.

[23] A. Chen, A.-V. Pham and R. I. Leoni, "A Novel Broadband Even-Mode Matching Network for Marchand Baluns," *Microwave Theory and Techniques, IEEE Transactions on,* vol. 57, no. 12,

pp. 2973-2980, 2009.

[24] Y.-L. Chen and H.-H. Lin, "Novel Broadband Planar Balun Using Multiple Coupled Lines," in *Microwave Symposium Digest, 2006. IEEE MTT-S International*, 2006.

[25] Z.-Y. Zhang, Y.-X. Guo, L. Ong and M. Y. W. Chia, "A new planar Marchand balun," in *Microwave Symposium Digest, 2005 IEEE MTT-S International*, 2005.

[26] C. Microsystems, *Getting Started Guide:The LTCC Shuttle Run*, 2012.

[27] P. Saad, M. Thorsell, K. Andersson and C. Fager, "Investigation of Push-Pull Microwave Power Amplifiers Using an Advanced Measurement Setup," *Microwave and Wireless Components Letters, IEEE,* vol. 23, no. 4, pp. 220-222, 2013.

[28] R. Smith, J. Lees, P. Tasker, J. Benedikt and S. Cripps, "A 40W push-pull power amplifier for high efficiency, decade bandwidth applications at microwave frequencies," in *Microwave Symposium Digest (MTT), 2012 IEEE MTT-S International*, 2012.

[29] H. Ta, A. Stameroff and A.-V. Pham, "Development of a defected ground structure wide bandwidth balun on multilayer organic substrate," in *Microwave Conference Proceedings (APMC), 2010 Asia-Pacific*, 2010.